



**Quasi-Static Uniaxial Tension Characteristics of
Plain-Woven Kevlar KM2 Fabric**

by Martin N. Raftenberg and Thomas J. Mulkern

ARL-TR-2891

December 2002

NOTICES

Disclaimers

The findings in this report are not to be construed as an official Department of the Army position unless so designated by other authorized documents.

Citation of manufacturer's or trade names does not constitute an official endorsement or approval of the use thereof.

Destroy this report when it is no longer needed. Do not return it to the originator.

Army Research Laboratory

Aberdeen Proving Ground, MD 21005-5066

ARL-TR-2891

December 2002

Quasi-Static Uniaxial Tension Characteristics of Plain-Woven Kevlar KM2 Fabric

**Martin N. Raftenberg and Thomas J. Mulkern
Weapons and Materials Research Directorate, ARL**

Contents

List of Figures	ii
List of Tables	iv
1. Introduction	1
2. Description of the Experiments	3
3. Results	3
3.1 Force-Displacement Curves	3
3.2 Initial Effective Ply Thickness	3
3.3 First Piola-Kirchhoff Stress	7
3.4 Fabric Work per Cross-Sectional Area	8
3.5 Fabric Strength and Displacement and Work at Failure	9
4. Analytical Fits to the Fabric Stress-Crosshead Displacement Curves	11
4.1 Bilinear Fit	11
4.2 Exponential Fit	14
4.3 Quartic Fit	21
5. Discussion	26
5.1 Force-Displacement Curves	26
5.2 Force-to-Stress Conversion	28
5.3 Fabric Strength	28
5.4 Failure Conditions for Warp vs. Fill Directions	29
5.5 Bilinear vs. Exponential vs. Quartic Fits to Stress-Displacement Curves	29
6. Concluding Remarks	31
6.1 Summary of Results	31
6.2 Recommendations for Future Work	31
7. References	32

List of Symbols	33
Report Documentation Page	35

List of Figures

Figure 1. The PPTA monomer that comprises Kevlar.....	2
Figure 2. A plain-weave structure consisting of mutually orthogonal families of warp and fill yarns.....	2
Figure 3. Instron 4505 loading frame.	4
Figure 4. An Instru-Met capstan webbing grip used in the tests.	5
Figure 5. A specimen clamped in the Instron 4505 apparatus.....	5
Figure 6. Applied force-crosshead displacement data from six specimens pulled in uniaxial tension along the warp direction.	6
Figure 7. Applied force-crosshead displacement data from six specimens pulled in uniaxial tension along the fill direction.	6
Figure 8. Fabric stress-crosshead displacement results from six specimens pulled in uniaxial tension along the warp direction.	7
Figure 9. Fabric stress-crosshead displacement results from six specimens pulled in uniaxial tension along the fill direction.	7
Figure 10. Work per cross-sectional area-crosshead displacement results from six specimens pulled in uniaxial tension along the warp direction.	8
Figure 11. Work per cross-sectional area-crosshead displacement results from six specimens pulled in uniaxial tension along the fill direction.	8
Figure 12. Fabric strength (first Piola-Kirchhoff stress at failure) for the 12 tests.....	9
Figure 13. Crosshead displacements at failure for the 12 tests.....	10
Figure 14. Work at failure per cross-sectional area for the 12 tests.	10
Figure 15. Sketch of a typical force-displacement curve for a fabric loaded in uniaxial tension.....	12
Figure 16. The bilinear fabric stress-crosshead displacement curve of equation 3.	13
Figure 17. Least-squares error vs. locking strain for test W1; the value of Δx_{lock} that minimizes ε was selected.	14
Figure 18. The small-displacement slope of the bilinear fit to the fabric stress-crosshead displacement results from each of the 12 tests.....	15
Figure 19. The large-displacement slope of the bilinear fit to the fabric stress-crosshead displacement results from each of the 12 tests.....	15

Figure 20. The locking displacement of the bilinear fit to the fabric stress-crosshead displacement results from each of the 12 tests.....	16
Figure 21. Least-square errors for bilinear fits to the fabric stress-crosshead displacement results from the 12 tests.	16
Figure 22. Bilinear fit to the fabric stress-crosshead displacement data from test W1.	18
Figure 23. Bilinear fit to the fabric stress-crosshead displacement data from test F1.....	18
Figure 24. Characteristic-stress parameter of the exponential fit to the fabric stress-crosshead displacement results from each of the 12 tests.....	19
Figure 25. Characteristic-length parameter of the exponential fit to the fabric stress-crosshead displacement results from each of the 12 tests.....	20
Figure 26. Least-square errors for exponential fits to the fabric stress-crosshead displacement results from the 12 tests.	20
Figure 27. Exponential fit to the fabric stress-crosshead displacement data from test W1.	22
Figure 28. Exponential fit to the fabric stress-crosshead displacement data from test F1.....	22
Figure 29. The linear-term coefficient for the quartic fits to the fabric stress-crosshead displacement data from the 12 tests.....	23
Figure 30. The quadratic-term coefficient for the quartic fits to the fabric stress-crosshead displacement data from the 12 tests.....	24
Figure 31. The cubic-term coefficient for the quartic fits to the fabric stress-crosshead displacement data from the 12 tests.....	24
Figure 32. The quartic-term coefficient for the quartic fits to the fabric stress-crosshead displacement data from the 12 tests.....	25
Figure 33. Least-square errors for quartic fits to the fabric stress-crosshead displacement results from the 12 tests.	25
Figure 34. Quartic fit to the fabric stress-crosshead displacement data from test W1.	27
Figure 35. Quartic fit to the fabric stress-crosshead displacement data from test F1.....	27
Figure 36. Least-squares errors for the bilinear, exponential, and quartic fits to the warp-direction fabric stress-crosshead displacement curves.	30
Figure 37. Least-squares errors for the bilinear, exponential, and quartic fits to the fill-direction fabric stress-crosshead displacement curves.	30

List of Tables

Table 1. Tensile properties of Kevlar yarns.....	1
Table 2. Properties of the specimens and tests.	6
Table 3. Failure conditions for the six warp tests.	11
Table 4. Failure conditions for the six fill tests.	11
Table 5. Parameters for bilinear fits to stress-displacement curves from the six warp tests.	17
Table 6. Parameters for bilinear fits to stress-displacement curves from the six fill tests.....	17
Table 7. Parameters for exponential fits to stress-displacement data from the six warp tests.	21
Table 8. Parameters for exponential fits to stress-displacement data from the six fill tests.	21
Table 9. Parameters for quartic fits to stress-displacement data from the six warp tests.	26
Table 10. Parameters for quartic fits to stress-displacement data from the six fill tests.....	26

1. Introduction

Plies of plain-woven Kevlar* aramid fabrics are the usual components of soft body armor (types I through III-A, as defined in National Institute of Justice [1987]). According to E. I. du Pont de Nemours and Company (DuPont) (undated), “Kevlar KM2 is a new, very high strength, high toughness (form of Kevlar) designed for improved ballistic fragmentation resistance and energy absorption capacity.” Table 1 compares single-yarn mechanical properties of KM2 to those of other forms of Kevlar. The KM2 properties in this table were obtained from publications by H. H. Yang of DuPont. Kevlar KM2, 29, 49, etc., are all composed of the same paraphenylene terephthalamide (PPTA) monomer shown in Figure 1. These different forms of Kevlar differ in the degree of crystallinity, which reflects the degree of molecular alignment and hydrogen bonding between neighboring molecules (Scott 2001). In Table 1, E_y is the yarn stiffness, or slope of a quasi-static, tensile stress-strain curve; $\sigma_{y,fail}$ is the yarn *strength*, or maximum stress attained on a tensile stress-strain curve; and $e_{y,fail}$ is the strain corresponding to maximum stress. Note that KM2 is distinguished by relatively large values for both $\sigma_{y,fail}$ and $e_{y,fail}$, which translates into a large value for toughness, or work per unit volume at failure.

Table 1. Tensile properties of Kevlar yarns.

Yarn Type	E_y (GPa)	$\sigma_{y,fail}$ (GPa)	$e_{y,fail}$
Kevlar 29 ^a	70	2.9	0.036
Kevlar 49 ^a	135	2.9	0.028
Kevlar 68 ^a	99	3.1	0.033
Kevlar 119 ^a	55	3.1	0.044
Kevlar 129 ^a	99	3.4	0.033
Kevlar 149 ^a	143	2.3	0.015
KM2 ^b	63	3.3	0.040

^a Yang (1993), p. 26.

^b Yang (2000), p. 219.

A single ply of plain-woven fabric consists of two mutually orthogonal families of yarns: one called “warp” and the other called “fill” (Figure 2). In the present study, single plies of plain-woven 600-denier Kevlar KM2 (style 706) were tested under quasi-static uniaxial tension. Twelve specimens were tested; six were loaded along the warp yarn direction and six along the fill yarn direction.

Section 2 describes the experimental procedure. The immediate data were applied force and crosshead displacement of the Instron machine. In section 3, these data are presented and

* Kevlar is a registered trademark of E. I. du Pont de Nemours and Company.

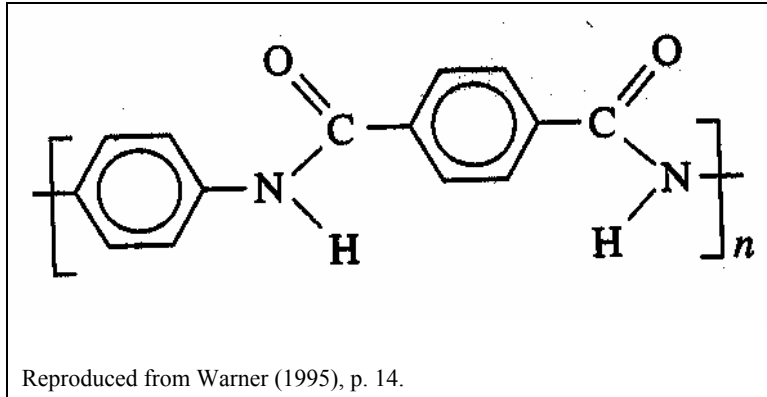


Figure 1. The PPTA monomer that comprises Kevlar.

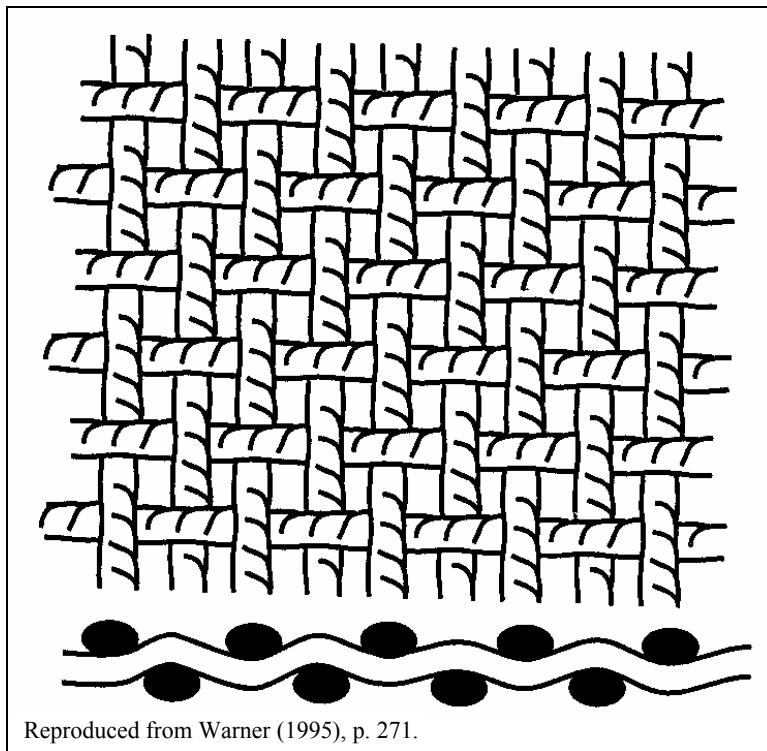


Figure 2. A plain-weave structure consisting of mutually orthogonal families of warp and fill yarns.

processed to obtain fabric stress-crosshead displacement curves. In the process, warp and fill values for fabric strength, σ_{fail} , are obtained. Least-squared-error fits to the stress-displacement curves are presented in section 4. Fits are obtained in three forms: (1) three-parameter bilinear curves, (2) two-parameter exponentials, and (3) four-parameter quartics. Sections 5 and 6 follow with discussions and conclusions, respectively.

2. Description of the Experiments

The uniaxial tension tests were performed under the guidance of American Society for Testing and Materials (ASTM) standard D5035-95 (ASTM 1995). An Instron 4505 load frame, such as that shown in Figure 3, was used (Instron Corporation 1988). The Instron load cell was rated at 100-kN maximum load. Instru-Met capstan webbing grips (Figure 4) were employed in place of the “wedge action grips” in Figure 3. Figure 5 shows a specimen clamped in preparation for a test.

All specimens were cut from the same sheet of style 706 fabric obtained from Hexcel Schwebel. Each specimen had an initial length of 1.219 m and an initial width, w_o , of 50.8 mm (Table 2). At each end of the specimen, a length of 50 mm was clamped into the capstan grip. The specimen was then wrapped twice around each capstan grip. During each test, the load frame crosshead speed was constant at 2.12 mm/s. This quantity is denoted dx/dt , where x is the distance between the moving and stationary crossheads at time t . The applied force was sampled 25 times/s.

Twelve specimens were tested. Six were elongated along the warp direction and had the fill direction associated with the width. These are tests W1–W6. The other six were elongated along the fill direction and had the warp direction associated with the width. These are denoted tests F1–F6.

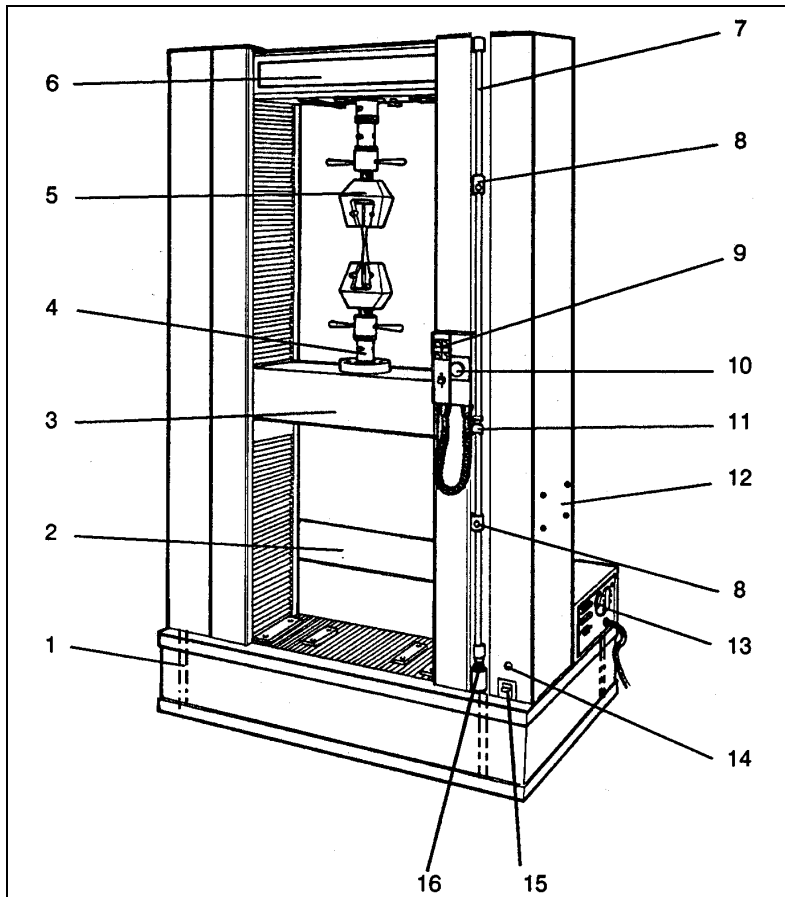
3. Results

3.1 Force-Displacement Curves

The quantities directly measured were the crosshead displacement, Δx , and the corresponding force, F , both as functions of time t . Data for Δx and F are plotted in Figures 6 and 7.

3.2 Initial Effective Ply Thickness

Calculation of first Piola-Kirchhoff stress, σ , from force F requires an evaluation of the ply’s initial thickness, d_o . This quantity does not admit a direct measurement because of the ply’s woven geometry. Instead, it was estimated based on three facts: (1) A ply of style 706 KM2 contains 34 yarns/in (Scott 2001), or 1.339 yarns/mm width; (2) A yarn of 600-denier KM2 contains 400 filaments (Scott 2001), hence, a ply of style 706 600-denier KM2 contains 535.4 filaments/mm width; and (3) A single filament has a circular cross section and a nominal diameter of 12 μm (Yang 1993, pp. 28 and 30), which corresponds to a filament cross-sectional area of $1.13 \times 10^{-4} \text{ (mm)}^2$. Hence, a single ply of style 706 600-denier KM2 has a cross-sectional area of $0.0606 \text{ (mm)}^2/\text{mm}$ width. This constitutes an effective thickness, d_o , of 60.6 μm , which is added to Table 2.



- 1 Levelling Adjusting Feet (one at each corner)
- 2 Rear Cover
- 3 Moving Crosshead
- 4 Load Cell
- 5 Wedge Action Grips (option)
- 6 Fixed Crosshead
- 7 Limits Rod
- 8 Limit Stop (Upper and Lower)
- 9 Handset Controls
- 10 Emergency Stop Button
- 11 Limit Adjustment Screw
- 12 Mounting Holes for Support Arm Assembly
(also available on left-hand side)
- 13 Frame Interconnection Panel
- 14 A.C. Mains Indicator
- 15 A.C. Mains On/Off Switch/Breaker
- 16 Limit Flag Adjustment Block

Reproduced from Instron Corporation (1988), pp. 1-4 and 1-5.

Figure 3. Instron 4505 loading frame.



Figure 4. An Instru-Met capstan webbing grip used in the tests.



Figure 5. A specimen clamped in the Instron 4505 apparatus.

Table 2. Properties of the specimens and tests.

w_o (mm)	dx/dt (mm/s)	d_o (μm)
50.8	2.12	60.6

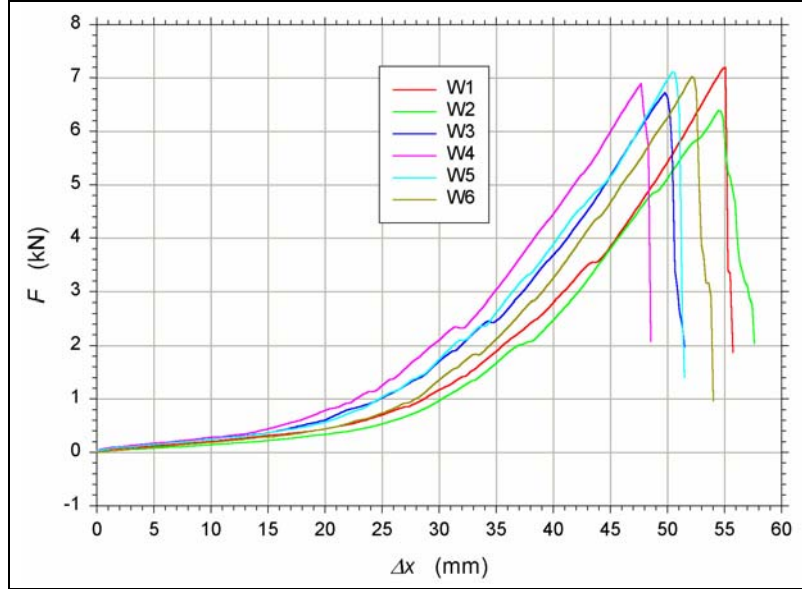


Figure 6. Applied force-crosshead displacement data from six specimens pulled in uniaxial tension along the warp direction.

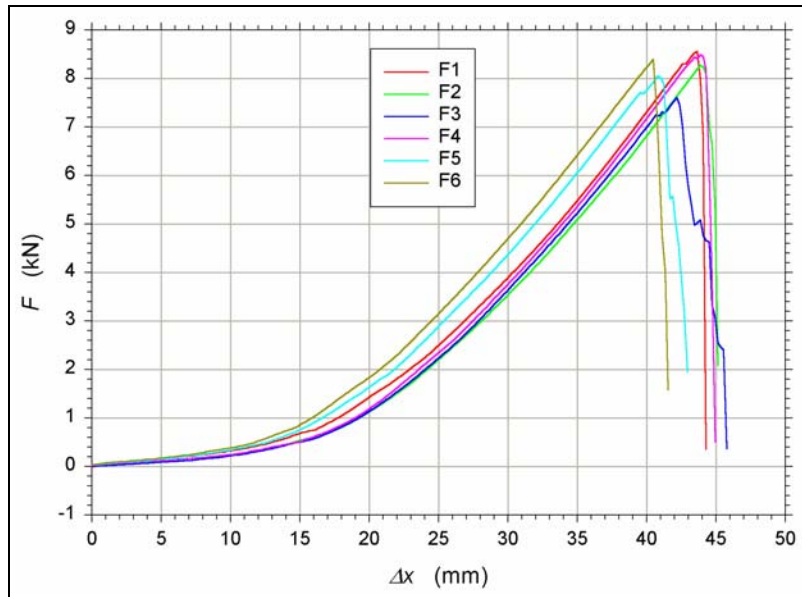


Figure 7. Applied force-crosshead displacement data from six specimens pulled in uniaxial tension along the fill direction.

3.3 First Piola-Kirchhoff Stress

Engineering stress, σ , can now be evaluated with the relationship

$$\sigma = \frac{F}{w_o d_o}. \quad (1)$$

Engineering stress is a component of the first Piola-Kirchhoff stress tensor (Malvern 1969, p. 222). The values for w_o and d_o in Table 2 were used to produce the fabric stress-crosshead displacement curves in Figures 8 and 9.

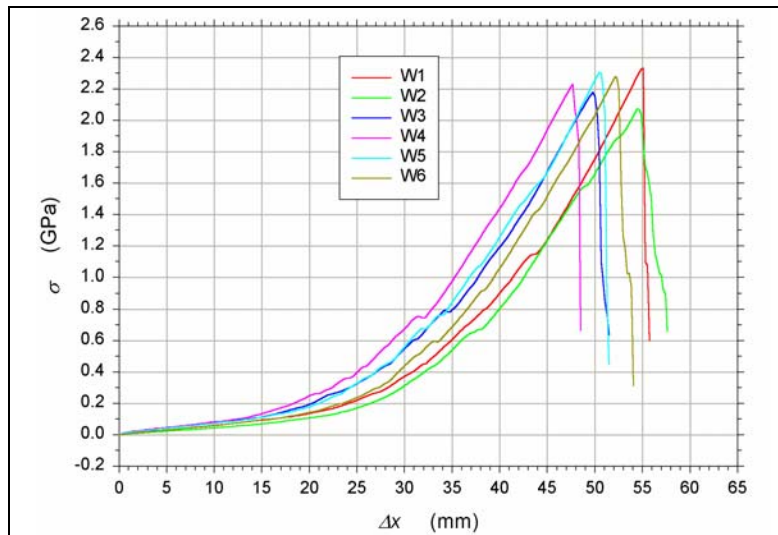


Figure 8. Fabric stress-crosshead displacement results from six specimens pulled in uniaxial tension along the warp direction.

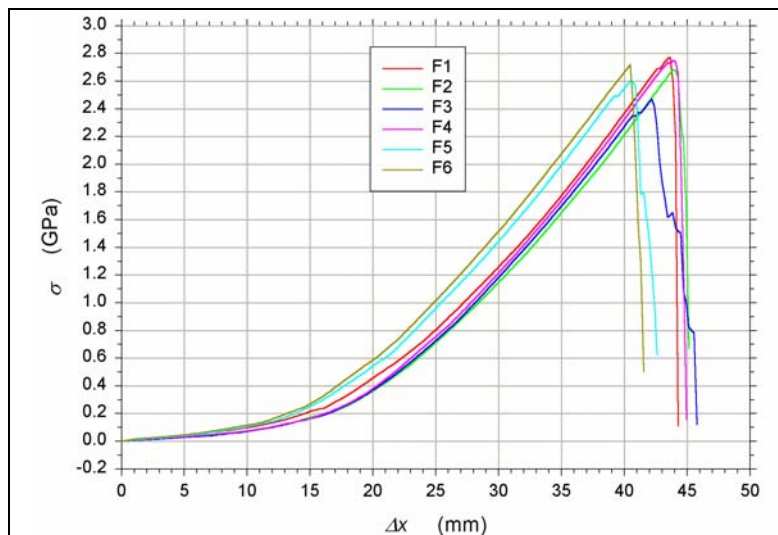


Figure 9. Fabric stress-crosshead displacement results from six specimens pulled in uniaxial tension along the fill direction.

3.4 Fabric Work per Cross-Sectional Area

Let W denote the fabric work per unit undeformed cross-sectional area, cumulative up to a given level of crosshead displacement Δx , or

$$W = \int_{x_0}^{x_0 + \Delta x} \sigma dx . \quad (2)$$

Numerical integration was performed by the trapezoid rule. Results are presented in Figures 10 and 11.

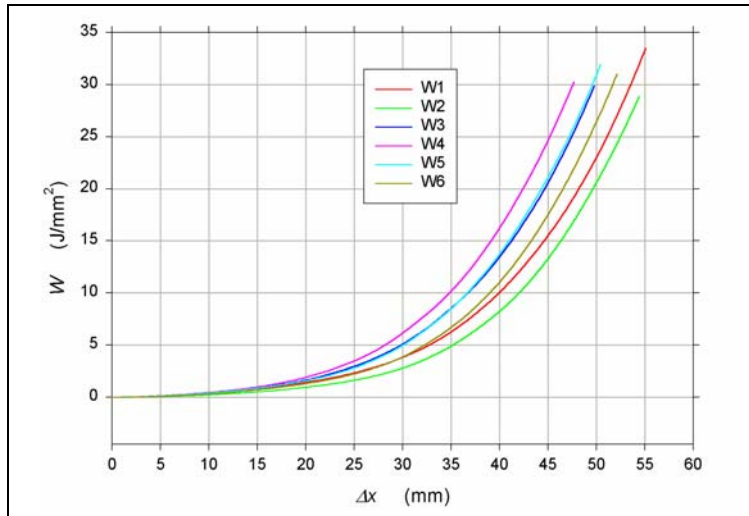


Figure 10. Work per cross-sectional area-crosshead displacement results from six specimens pulled in uniaxial tension along the warp direction.

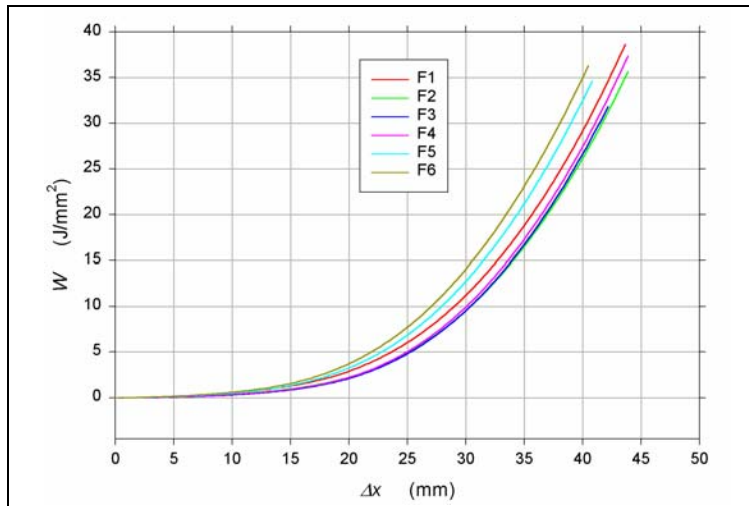


Figure 11. Work per cross-sectional area-crosshead displacement results from six specimens pulled in uniaxial tension along the fill direction.

3.5 Fabric Strength and Displacement and Work at Failure

For a given test, the *strength*, or maximum value attained by the first Piola-Kirchhoff stress, is denoted by σ_{fail} . Visible degradation to the specimen, in the form of slack and pulled-out yarns, became apparent at about the time at which maximum stress was reached, hence, the use of the subscript “fail.” The corresponding values of crosshead displacement and work per area are denoted by Δx_{fail} and W_{fail} , respectively. Note that W_{fail} is proportional to toughness, or the work at failure per unit volume. The quantities σ_{fail} , Δx_{fail} , and W_{fail} are plotted in Figures 12–14, respectively, and listed in Tables 3 and 4. Mean values, averaged over six tests, for the strength were 2.23 GPa for the warp direction and 2.67 GPa for the fill direction.

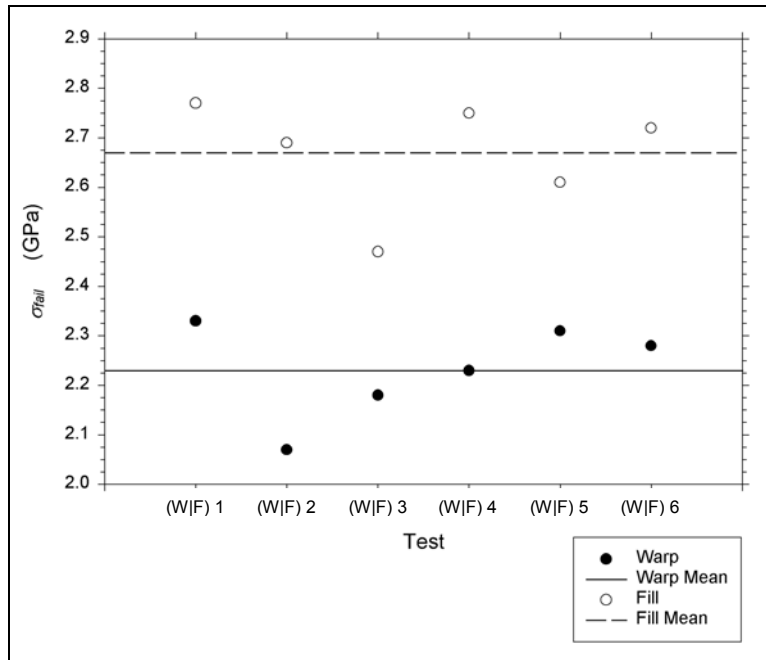


Figure 12. Fabric strength (first Piola-Kirchhoff stress at failure) for the 12 tests.

The specimens loaded along the warp direction consistently exhibited smaller strength (failure stresses) and larger failure displacements than those specimens loaded along the fill direction. The work per area at failure showed percentage-wise less systematic difference between warp and fill, although five fill specimens required more work to fail than did any of the six warp specimens.

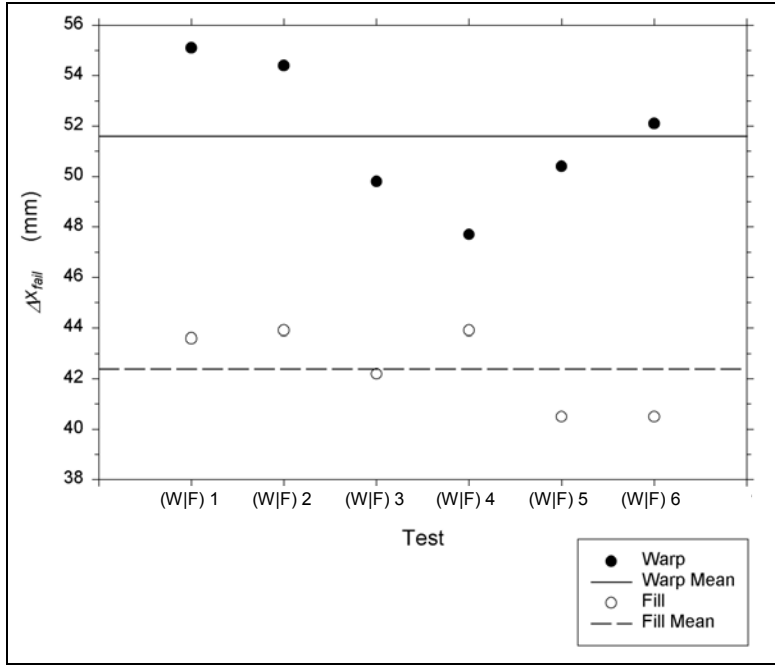


Figure 13. Crosshead displacements at failure for the 12 tests.

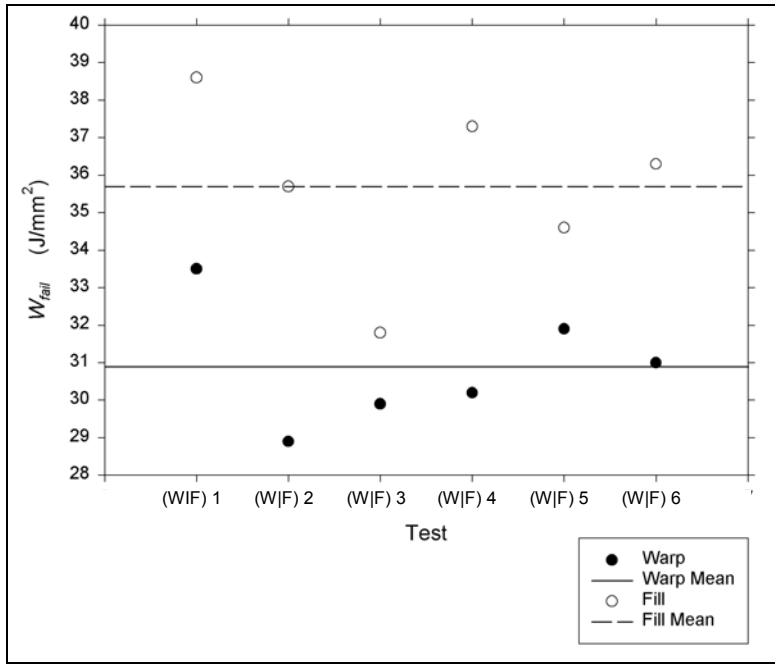


Figure 14. Work at failure per cross-sectional area for the 12 tests.

Table 3. Failure conditions for the six warp tests.

Test	σ_{fail}^a (GPa)	Δx_{fail}^b (mm)	W_{fail}^c (J/mm ²)
W1	2.33	55.1	33.5
W2	2.07	54.4	28.9
W3	2.18	49.8	29.9
W4	2.23	47.7	30.2
W5	2.31	50.4	31.9
W6	2.28	52.1	31.0
Mean	2.23	51.6	30.9
Standard deviation	0.10	2.8	1.6

^aPlotted in Figure 12.

^bPlotted in Figure 13.

^cPlotted in Figure 14.

Table 4. Failure conditions for the six fill tests.

Test	σ_{fail}^a (GPa)	Δx_{fail}^b (mm)	W_{fail}^c (J/mm ²)
F1	2.77	43.6	38.6
F2	2.69	43.9	35.7
F3	2.47	42.2	31.8
F4	2.75	43.9	37.3
F5	2.61	40.5	34.6
F6	2.72	40.5	36.3
Mean	2.67	42.4	35.7
Standard deviation	0.11	1.6	2.4

^aPlotted in Figure 12.

^bPlotted in Figure 13.

^cPlotted in Figure 14.

4. Analytical Fits to the Fabric Stress-Crosshead Displacement Curves

4.1 Bilinear Fit

According to Grosberg (1969), Figure 15 sketches a force-displacement curve obtained for a generic fabric. The curve has three regions: (1) an initial nonlinear (negative-curvature) region primarily governed by “inter-fiber friction,” (2) an intermediate nonlinear (positive-curvature) region corresponding to the phenomenon of fiber uncrimping, and (3) a final linear region that reflects the stiffness associated with the elongation of uncrimped yarns. The curve abruptly terminates at the end of this third region, corresponding to failure of the fabric.

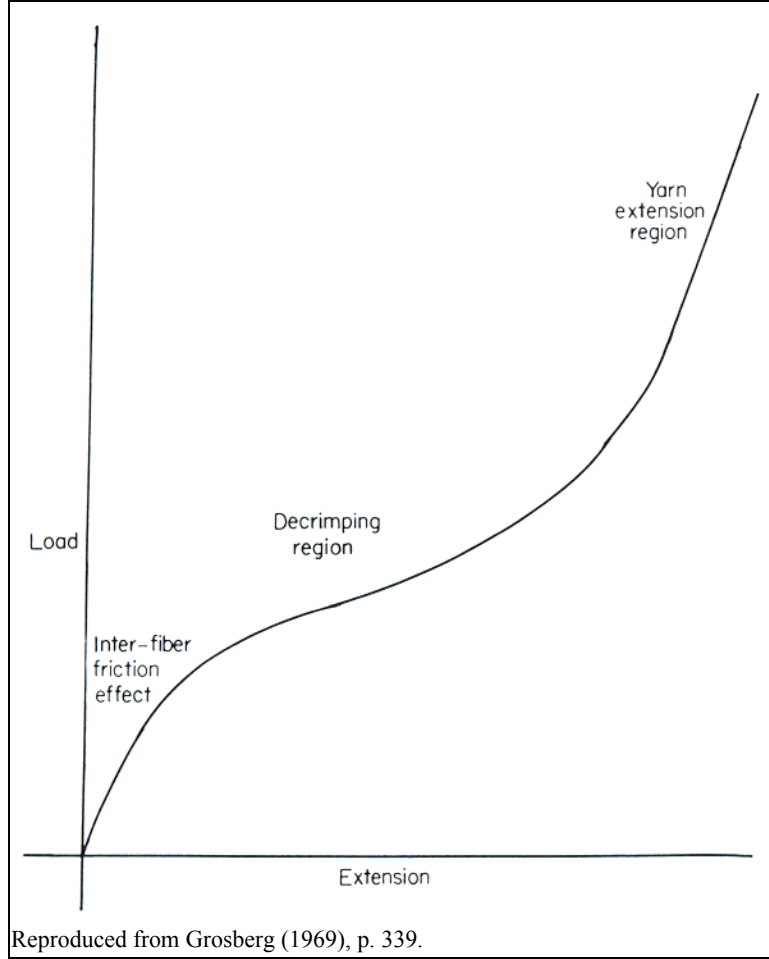


Figure 15. Sketch of a typical force-displacement curve for a fabric loaded in uniaxial tension.

In Figures 6 and 7, the warp and fill stress-displacement curves from a ply of 600-denier KM2 do not exhibit the initial negative-curvature region in Figure 15. Because of Kevlar's high strength, the initial negative-curvature region may be present but applicable to only a negligible fraction of the total load excursion.

The two-part stress-displacement curve sketched in Figure 16 consists of two linear portions joined at the locking displacement, Δx_{lock} . According to Jinlian and Newton (1993), this bilinear fit of Figure 16 (albeit applied to stress-strain rather than to stress-displacement) may have been first proposed by Alsawaf (1985). The slope of the small-displacement portion is denoted β_1 , and that of the large-displacement portion is denoted β_2 . The displacement corresponding to the maximum stress, at which failure is assumed to occur, is denoted Δx_{fail} . This bilinear stress-displacement curve is described by

$$\sigma = \begin{cases} \beta_1 \Delta x & ; 0 \leq \Delta x \leq \Delta x_{lock} \\ \beta_1 \Delta x_{lock} + \beta_2 (\Delta x - \Delta x_{lock}) & ; \Delta x_{lock} < \Delta x \leq \Delta x_{fail} \end{cases} \quad (3)$$

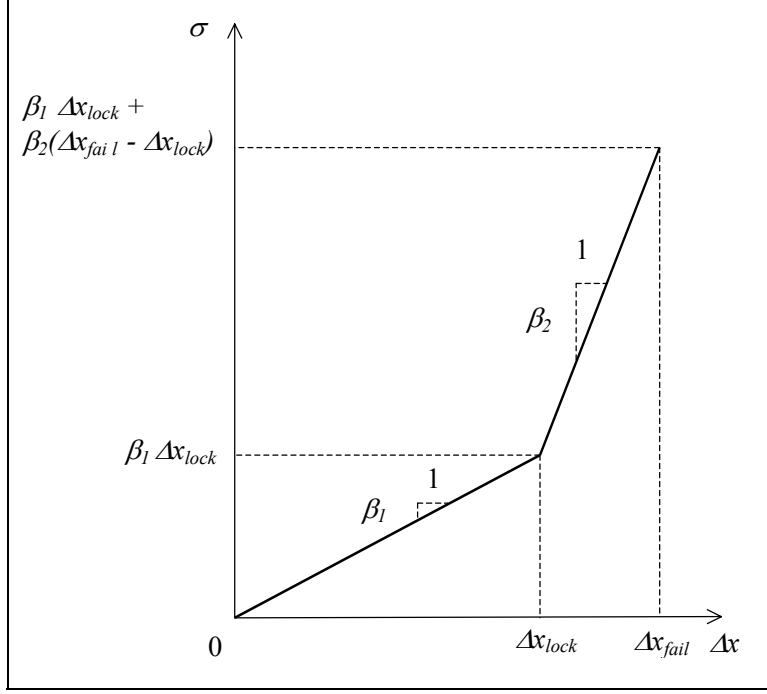


Figure 16. The bilinear fabric stress-crosshead displacement curve of equation 3.

Parameter Δx_{fail} is determined directly from the data (see Tables 3 and 4 and Figure 13). A least-squares-error procedure is used to obtain Δx_{lock} , β_1 , and β_2 for each of the 12 tests.

For a given test, all data at strains larger than Δx_{fail} are discarded. This leaves N points of measured data: $(\Delta x_i, \sigma_i)$, $i = 1, 2, \dots, N$, where

$$\Delta x_N = \Delta x_{fail} . \quad (4)$$

The procedure is to pick a Δx_{lock} that satisfies the condition

$$0 \leq \Delta x_{lock} \leq \Delta x_{fail} . \quad (5)$$

Define N_l by the conditions

$$\Delta x_{N_l} \leq \Delta x_{lock} ; \quad (6a)$$

$$\Delta x_{N_l+1} > \Delta x_{lock} . \quad (6b)$$

The total squared error of the fit is given by

$$\varepsilon^2(\beta_1, \beta_2; \Delta x_{lock}) = \sum_{i=1}^{N_l} (\beta_1 \Delta x_i - \sigma_i)^2 + \sum_{i=N_l+1}^N [\beta_1 \Delta x_{lock} + \beta_2 (\Delta x_i - \Delta x_{lock}) - \sigma_i]^2 . \quad (7)$$

The dependency of ε^2 on Δx_{lock} is partly embedded in the limits of summation. For a given Δx_{lock} , minimization of ε^2 with respect to β_1 and β_2 is imposed.

$$\frac{\partial \varepsilon^2}{\partial \beta_1} = 0, \quad \frac{\partial \varepsilon^2}{\partial \beta_2} = 0. \quad (8)$$

Δx_{lock} is then varied, covering the range of equation 5 in small increments. Minimization of ε with respect to Δx_{lock} is imposed graphically (Figure 17).

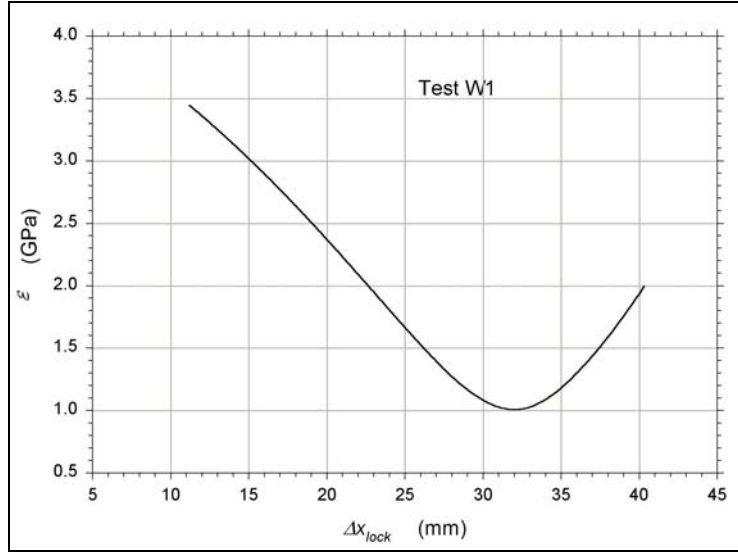


Figure 17. Least-squares error vs. locking strain for test W1; the value of Δx_{lock} that minimizes ε was selected.

The results for β_1 , β_2 , Δx_{lock} , and ε for the 12 tests are given in Figures 18–21, respectively, and in Tables 5 and 6. For illustration, the bilinear fits obtained for tests W1 and F1 are displayed in Figures 22 and 23, respectively.

Values for Δx_{lock} are consistently larger for warp than for fill. Values for β_2 are consistently smaller for warp than for fill. Values for β_1 are mixed with regard to warp and fill. Values for ε are consistently larger for warp than for fill, indicating that the bilinear form is a better description for the fill than for the warp response.

4.2 Exponential Fit

Consider the exponential fit to the entire fabric stress-crosshead displacement curve ($0 \leq \Delta x \leq \Delta x_{fail}$):

$$\sigma = \xi \left[\exp\left(\frac{\Delta x}{\eta}\right) - 1 \right]. \quad (9)$$

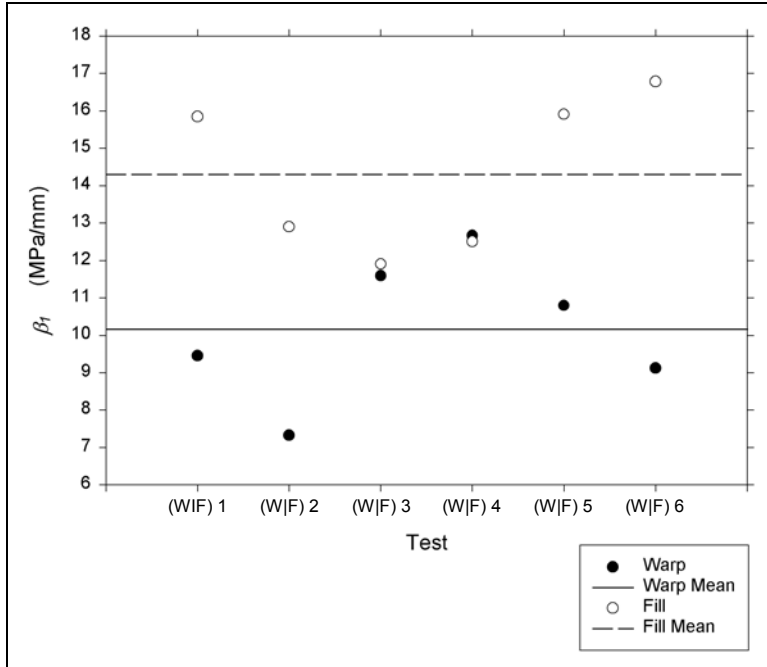


Figure 18. The small-displacement slope of the bilinear fit to the fabric stress-crosshead displacement results from each of the 12 tests.

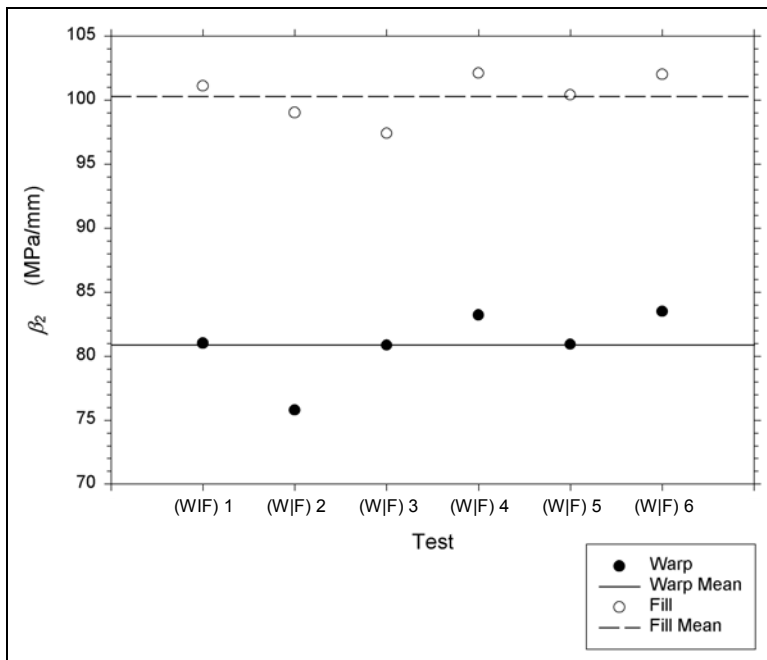


Figure 19. The large-displacement slope of the bilinear fit to the fabric stress-crosshead displacement results from each of the 12 tests.

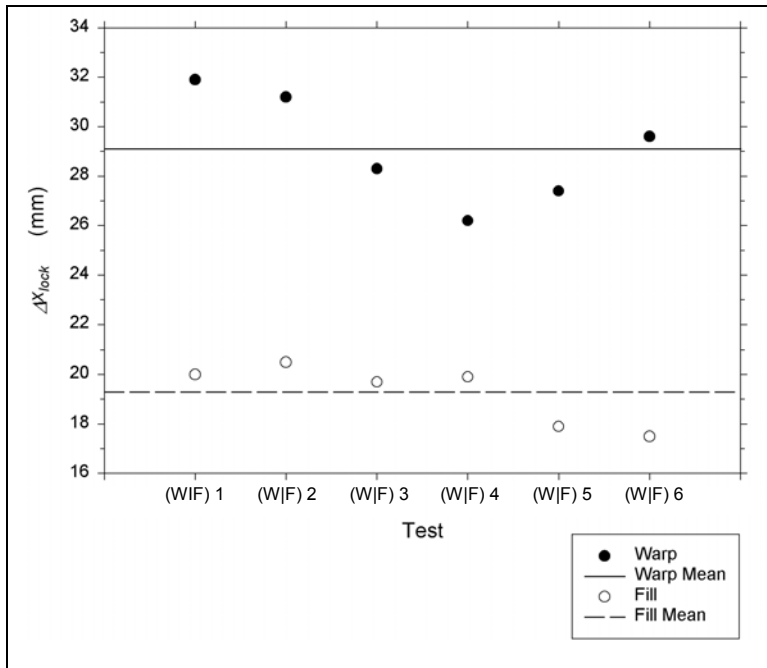


Figure 20. The locking displacement of the bilinear fit to the fabric stress-crosshead displacement results from each of the 12 tests.

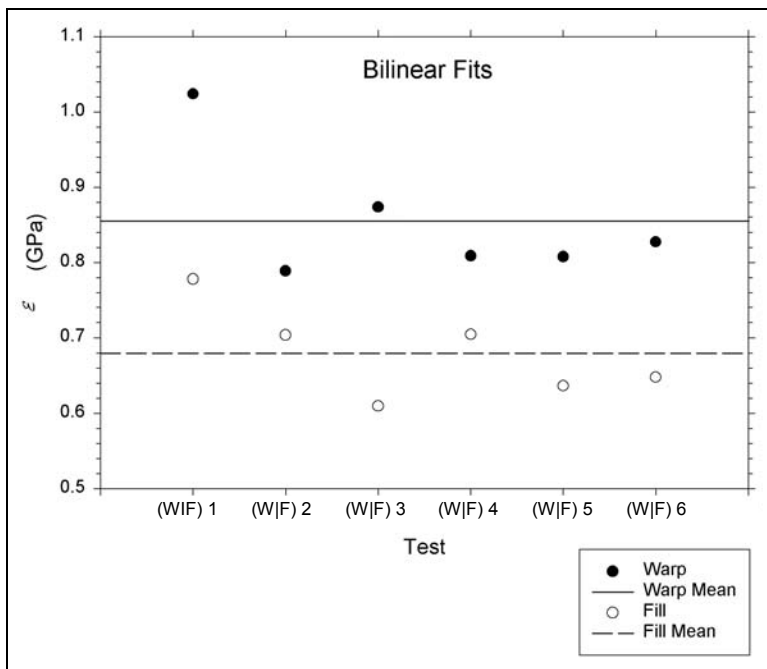


Figure 21. Least-square errors for bilinear fits to the fabric stress-crosshead displacement results from the 12 tests.

Table 5. Parameters for bilinear fits to stress-displacement curves from the six warp tests.

Test	β_1^a (MPa/mm)	β_2^b (MPa/mm)	Δx_{lock}^c (mm)	ε^d (GPa)
W1	9.455	81.02	31.9	1.024
W2	7.329	75.80	31.2	0.7887
W3	11.59	80.86	28.3	0.8737
W4	12.67	83.21	26.2	0.8089
W5	10.80	80.93	27.4	0.8076
W6	9.125	83.50	29.6	0.8273
Mean	10.16	80.89	29.1	0.855
Standard deviation	1.92	2.76	2.2	0.088

^aPlotted in Figure 18.

^bPlotted in Figure 19.

^cPlotted in Figure 20.

^dPlotted in Figure 21.

Table 6. Parameters for bilinear fits to stress-displacement curves from the six fill tests.

Test	β_1^a (MPa/mm)	β_2^b (MPa/mm)	Δx_{lock}^c (mm)	ε^d (GPa)
F1	15.85	101.1	20.0	0.7780
F2	12.90	99.02	20.5	0.7036
F3	11.91	97.41	19.7	0.6102
F4	12.51	102.1	19.9	0.7045
F5	15.91	100.4	17.9	0.6371
F6	16.78	102.0	17.5	0.6483
Mean	14.31	100.3	19.3	0.6803
Standard deviation	2.10	1.8	1.2	0.0608

^aPlotted in Figure 18.

^bPlotted in Figure 19.

^cPlotted in Figure 20.

^dPlotted in Figure 21.

This functional form seems to have been first proposed by Jinlian and Newton (1993). The two constants, ξ and η , remain to be determined by a least-squares-error procedure.

For a given test, the displacement corresponding to the maximum measured stress is denoted Δx_{fail} . All data at displacements larger than Δx_{fail} are then discarded. We are left with N points of measured data: $(\Delta x_i, \sigma_i)$, $i = 1, 2, \dots, N$, where

$$\Delta x_N = \Delta x_{fail} . \quad (10)$$

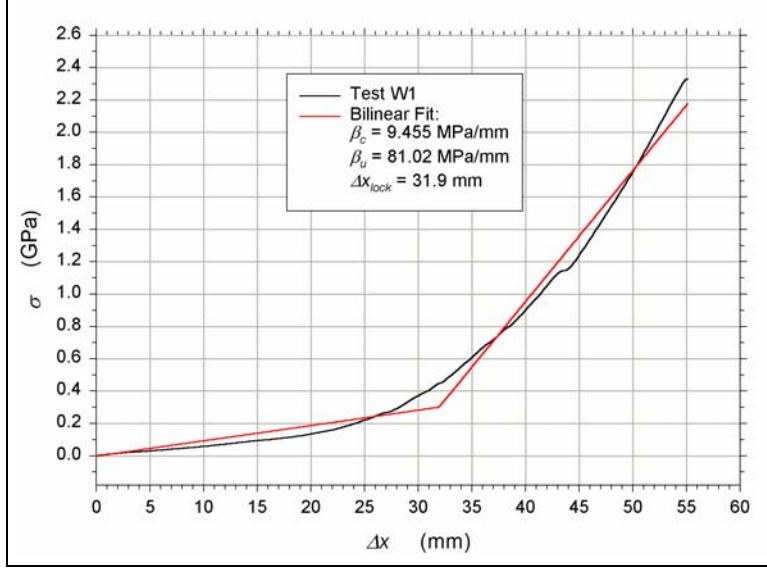


Figure 22. Bilinear fit to the fabric stress-crosshead displacement data from test W1.

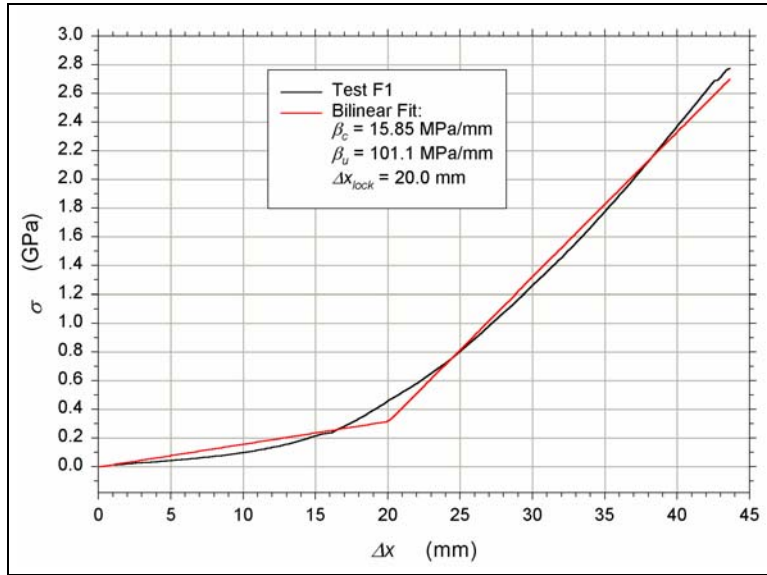


Figure 23. Bilinear fit to the fabric stress-crosshead displacement data from test F1.

The total squared error is

$$\varepsilon^2(\xi, \eta) = \sum_{i=1}^N \left\{ \xi \left[\exp\left(\frac{\Delta x_i}{\eta}\right) - 1 \right] - \sigma_i \right\}^2. \quad (11)$$

For each test, the particular set of values for ξ and η is found that minimizes the error ε . The minimization conditions

$$\frac{\partial \varepsilon^2}{\partial \xi} = 0, \quad \frac{\partial \varepsilon^2}{\partial \eta} = 0, \quad (12)$$

lead to two coupled nonlinear equations for ξ and η that can only be solved numerically. Instead, a “brute force” approach was applied, in which ξ and η were varied in small increments and the minimum in ε was sought. The results for ξ , η , and ε are given in Figures 24–26, respectively, and in Tables 7 and 8. The exponential fits to tests W1 and F1 are displayed in Figures 27 and 28, respectively.

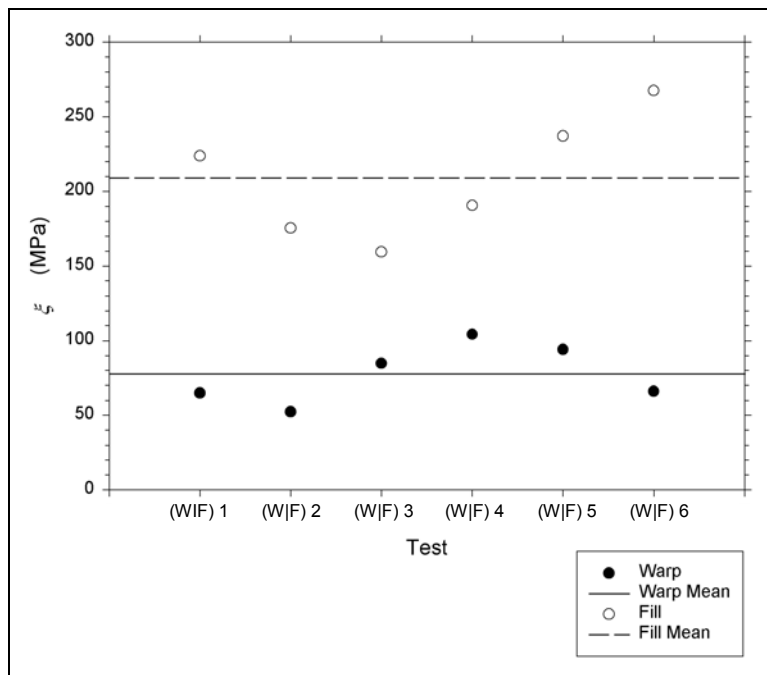


Figure 24. Characteristic-stress parameter of the exponential fit to the fabric stress-crosshead displacement results from each of the 12 tests.

Values for ξ are consistently smaller for warp than for fill. Values for η are also generally smaller for warp than for fill, although there is some overlap. Both of these observations reflect the generally smaller stress levels for warp than for fill for a given crosshead displacement.

Values for ε are consistently smaller for warp than for fill, indicating the exponential form to be more applicable to warp than to fill data. Recall from section 4.1 that the reverse was the case for the bilinear form.

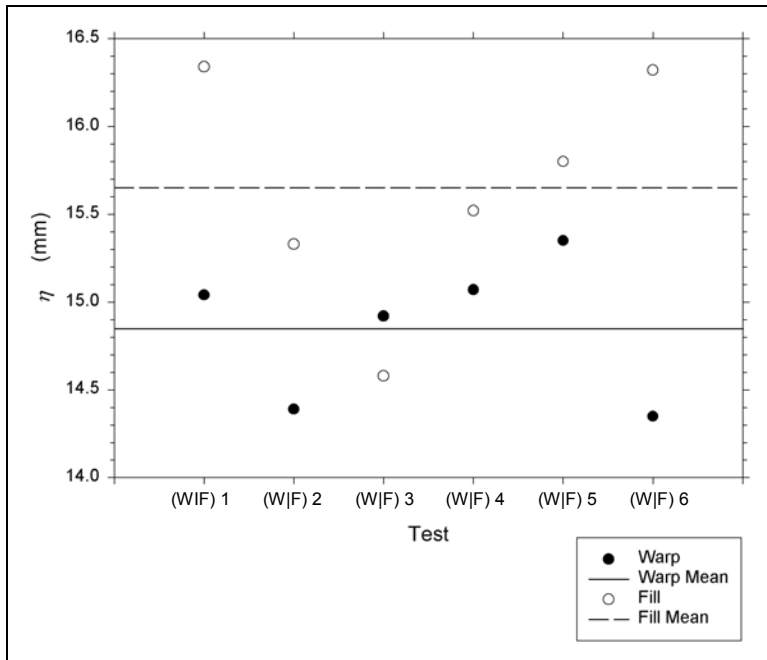


Figure 25. Characteristic-length parameter of the exponential fit to the fabric stress-crosshead displacement results from each of the 12 tests.

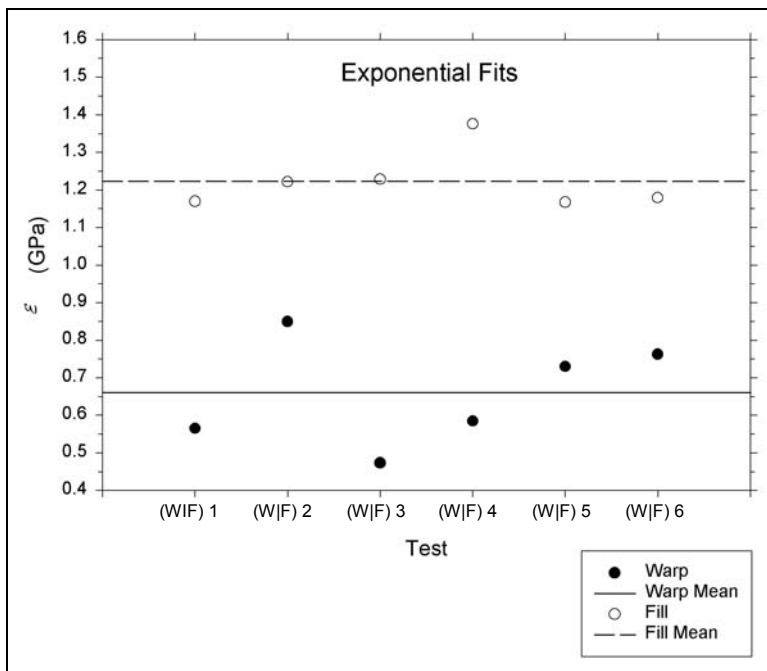


Figure 26. Least-square errors for exponential fits to the fabric stress-crosshead displacement results from the 12 tests.

Table 7. Parameters for exponential fits to stress-displacement data from the six warp tests.

Test	ξ^a (MPa)	η^b (mm)	ε^c (GPa)
W1	64.89	15.04	0.5656
W2	52.33	14.39	0.8494
W3	84.82	14.92	0.4731
W4	104.3	15.07	0.5847
W5	94.07	15.35	0.7299
W6	66.09	14.35	0.7630
Mean	77.8	14.85	0.6610
Standard deviation	19.8	0.40	0.1420

^aPlotted in Figure 24.

^bPlotted in Figure 25.

^cPlotted in Figure 26.

Table 8. Parameters for exponential fits to stress-displacement data from the six fill tests.

Test	ξ^a (MPa)	η^b (mm)	ε^c (GPa)
F1	223.7	16.34	1.170
F2	175.4	15.33	1.222
F3	159.5	14.58	1.229
F4	190.5	15.52	1.376
F5	237.0	15.80	1.167
F6	267.4	16.32	1.179
Mean	208.9	15.65	1.224
Standard deviation	40.8	0.67	0.079

^aPlotted in Figure 24.

^bPlotted in Figure 25.

^cPlotted in Figure 26.

4.3 Quartic Fit

Consider the quartic fit to the entire fabric stress-crosshead displacement curve ($0 \leq \Delta x \leq \Delta x_{fail}$),

$$\sigma = \alpha \Delta x + \beta(\Delta x)^2 + \gamma(\Delta x)^3 + \delta(\Delta x)^4 . \quad (13)$$

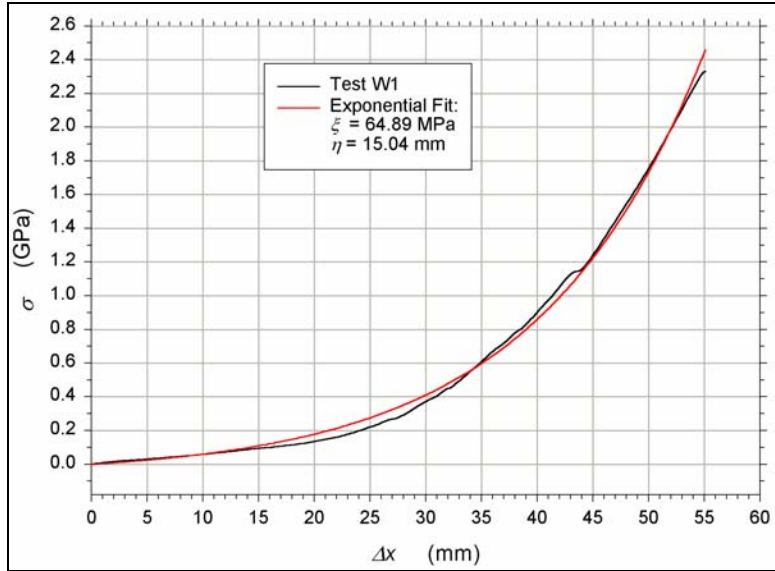


Figure 27. Exponential fit to the fabric stress-crosshead displacement data from test W1.

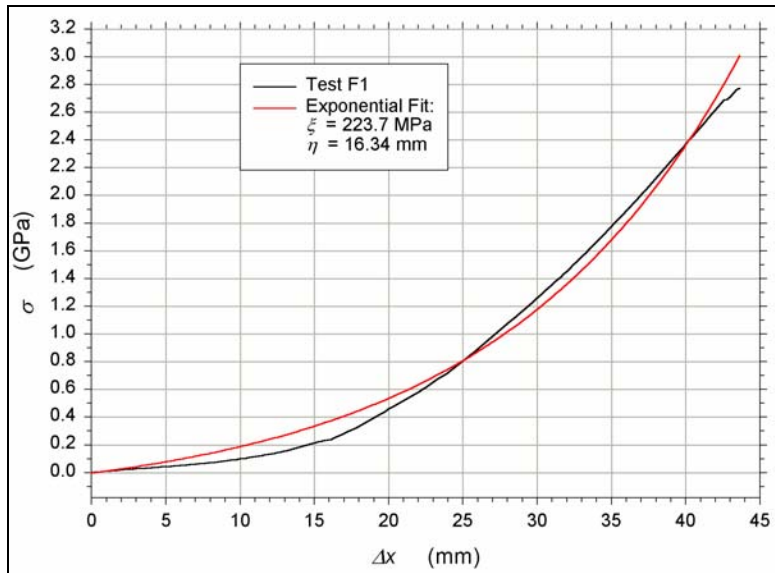


Figure 28. Exponential fit to the fabric stress-crosshead displacement data from test F1.

The authors know of no previous attempts to apply this quartic functional form to woven fabric data. The four constants, α , β , γ , and δ , remain to be determined by a least-squares-error procedure.

For a given test, the displacement corresponding to the maximum measured stress is denoted Δx_{fail} . All data at displacements larger than Δx_{fail} are then discarded. We are left with N points of measured data: $(\Delta x_i, \sigma_i)$, $i = 1, 2, \dots, N$, where

$$\Delta x_N = \Delta x_{fail} . \quad (14)$$

The total squared error is

$$\varepsilon^2(\alpha, \beta, \gamma, \delta) = \sum_{i=1}^N [\alpha \Delta x_i + \beta (\Delta x_i)^2 + \gamma (\Delta x_i)^3 + \delta (\Delta x_i)^4 - \sigma_i]^2 . \quad (15)$$

The four minimization conditions,

$$\frac{\partial \varepsilon^2}{\partial \alpha} = 0, \quad \frac{\partial \varepsilon^2}{\partial \beta} = 0, \quad \frac{\partial \varepsilon^2}{\partial \gamma} = 0, \quad \frac{\partial \varepsilon^2}{\partial \delta} = 0, \quad (16)$$

lead to four linear algebraic equations for α , β , γ , and δ . The results for α , β , γ , δ , and ε are given in Figures 29–33, respectively, and in Tables 9 and 10. The quartic fits obtained for tests W1 and F1 are displayed in Figures 34 and 35, respectively.

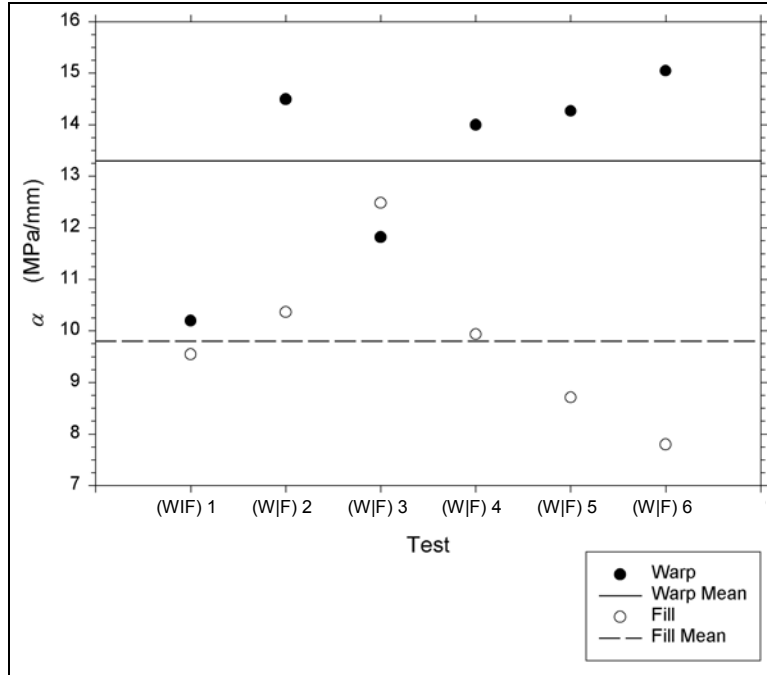


Figure 29. The linear-term coefficient for the quartic fits to the fabric stress-crosshead displacement data from the 12 tests.

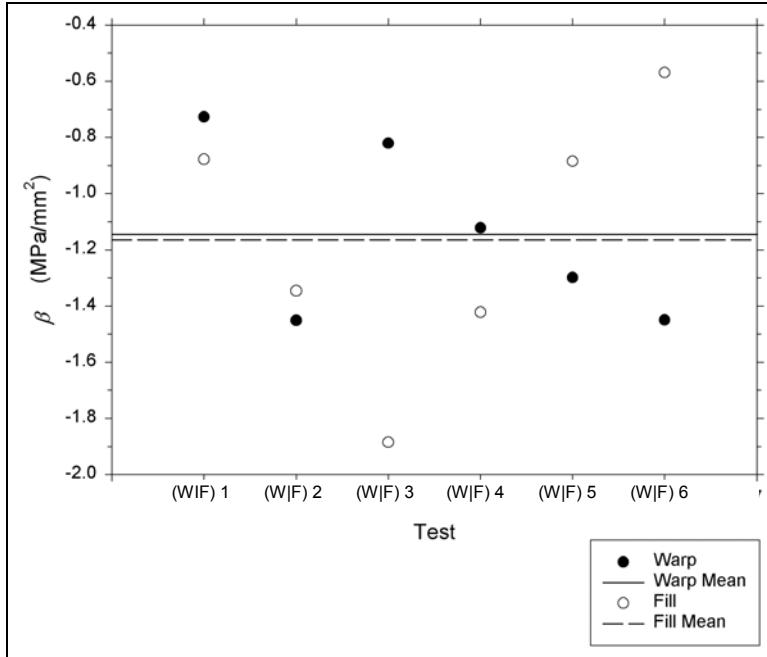


Figure 30. The quadratic-term coefficient for the quartic fits to the fabric stress-crosshead displacement data from the 12 tests.

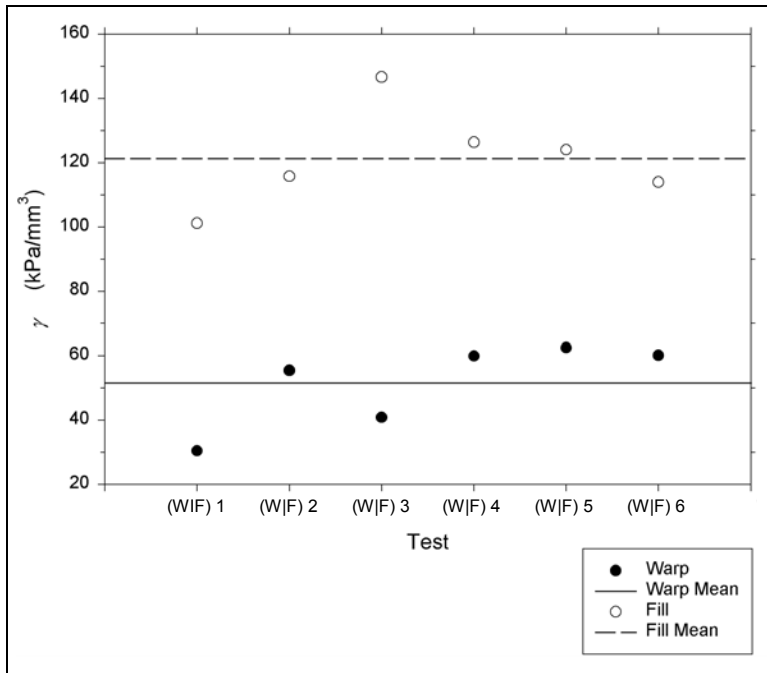


Figure 31. The cubic-term coefficient for the quartic fits to the fabric stress-crosshead displacement data from the 12 tests.

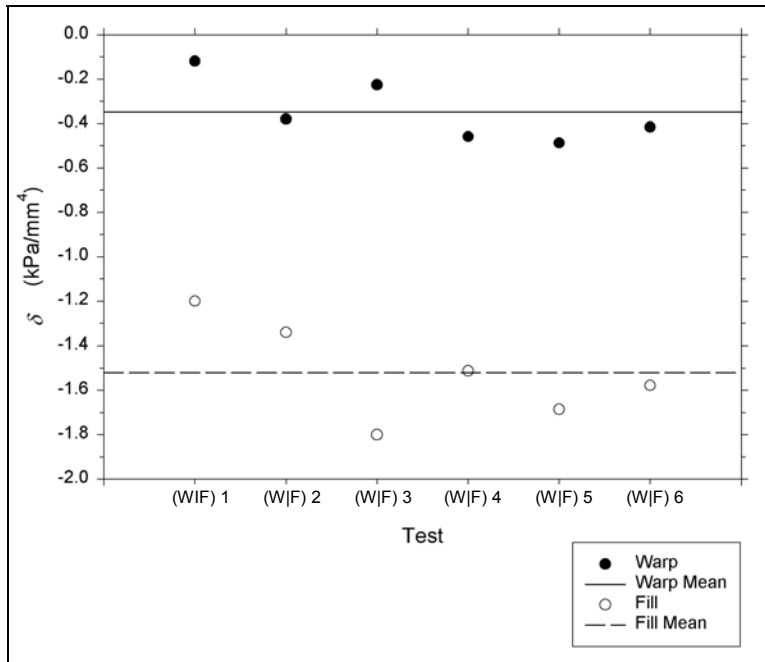


Figure 32. The quartic-term coefficient for the quartic fits to the fabric stress-crosshead displacement data from the 12 tests.

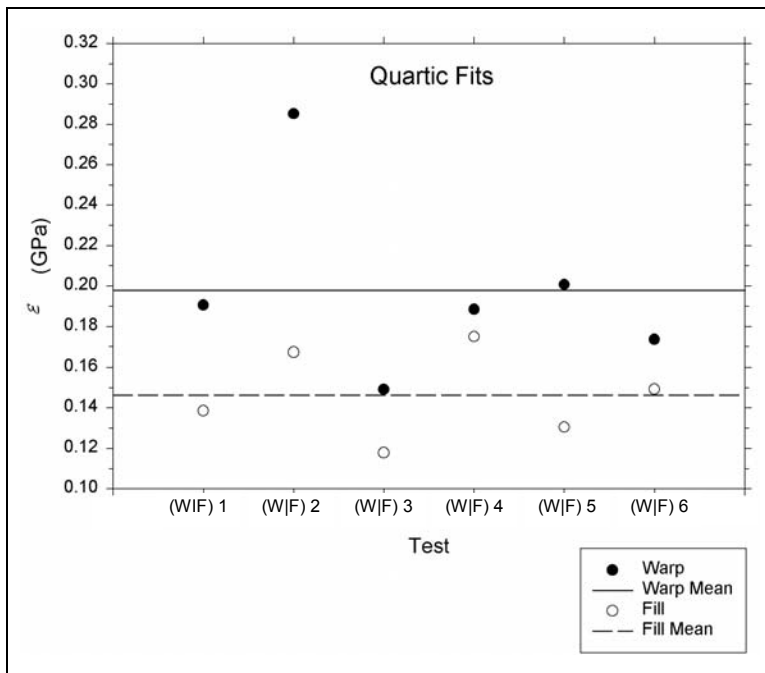


Figure 33. Least-square errors for quartic fits to the fabric stress-crosshead displacement results from the 12 tests.

Table 9. Parameters for quartic fits to stress-displacement data from the six warp tests.

Test	α^a (kPa/mm)	β^b (kPa/mm ²)	γ^c (kPa/mm ³)	δ^d (kPa/mm ⁴)	ε^e (GPa)
W1	10200	! 727.0	30.47	! 0.1186	0.1906
W2	14490	! 1451	55.49	! 0.3798	0.2853
W3	11820	! 820.2	40.86	! 0.2257	0.1492
W4	14000	! 1122	59.99	! 0.4589	0.1885
W5	14270	! 1298	62.52	! 0.4877	0.2008
W6	15050	! 1450	60.14	! 0.4160	0.1736
Mean	13300	! 1145	51.58	! 0.3478	0.1980
Standard deviation	1880	313	12.96	0.1449	0.0464

^aPlotted in Figure 29.

^bPlotted in Figure 30.

^cPlotted in Figure 31.

^dPlotted in Figure 32.

^ePlotted in Figure 33.

Table 10. Parameters for quartic fits to stress-displacement data from the six fill tests.

Test	α^a (kPa/mm)	β^b (kPa/mm ²)	γ^c (kPa/mm ³)	δ^d (kPa/mm ⁴)	ε^e (GPa)
F1	9546	! 877.6	101.1	! 1.200	0.1386
F2	10360	! 1346	115.7	! 1.341	0.1675
F3	12480	! 1885	146.6	! 1.800	0.1179
F4	9936	! 1422	126.3	! 1.513	0.1750
F5	8712	! 884.5	124.0	! 1.686	0.1306
F6	7796	! 569.2	113.9	! 1.578	0.1493
Mean	9810	! 1164	121.3	! 1.520	0.1465
Standard deviation	1600	476	15.3	0.221	0.0219

^aPlotted in Figure 29.

^bPlotted in Figure 30.

^cPlotted in Figure 31.

^dPlotted in Figure 32.

^ePlotted in Figure 33.

Values for γ are consistently larger in the fill tests than the warp tests. The reverse is true for δ . For α and β , no systematic relative orderings of warp and fill values are apparent. Values for ε are generally smaller for fill than for warp data fits, indicating that the quartic fit works somewhat better for fill data.

5. Discussion

5.1 Force-Displacement Curves

The force-crosshead displacement curves, discussed in section 3.1, from the six warp-direction tests (Figure 6) exhibit greater intertest variation than those from the six fill-direction tests (Figure 7). Such intertest variations for either warp or fill may reflect initial differences between

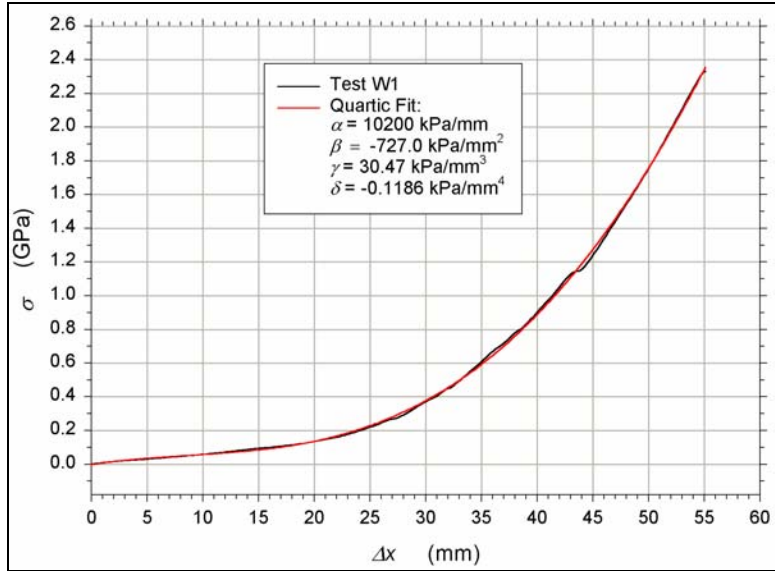


Figure 34. Quartic fit to the fabric stress-crosshead displacement data from test W1.

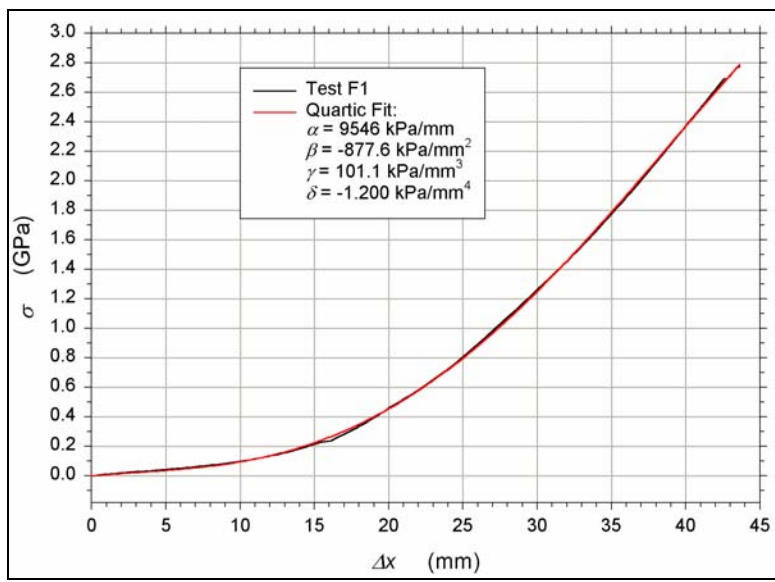


Figure 35. Quartic fit to the fabric stress-crosshead displacement data from test F1.

the six specimens. All 12 specimens were cut from a single sheet of KM2 obtained from Hexcel Schwebel, so that there is no reason to expect substantial interspecimen variations. Other possible sources for the differences between results from the six warp-direction tests are intertest differences in the degree of specimen slippage, yarn rotation, and/or nonuniform load distribution among the 68 yarns across the specimen's 50.8-mm width.

The force-displacement curve for each warp-direction test displays one or more jogs (Figure 6). Note that no such jogs are evident in the fill-direction tests (Figure 7). The most plausible explanation for these warp-direction jogs is sudden specimen slippage. One possible site for slippage was the clamps at either end. The two 50-mm-long clamped ends were not remeasured following the test, so slippage at the ends cannot be ruled out. A more likely type of slippage would have involved the sudden overcoming of frictional restraint somewhere along the two wrappings around either capstan.

Yarn rotation could have resulted from initial misalignment of the specimen, whereby the loading direction would not have coincided exactly with the direction of yarn orientation. The load's off-axis component would then have caused yarn rotation ("scissoring") with relatively little fabric resistance.

There is no apparent reason why either specimen slippage, yarn rotation, or nonuniform loading would have been more likely in the warp-direction tests than in the fill-direction tests. In fact, slippage, in particular, seems more likely in the fill direction because of greater strength, smaller elongation, and greater toughness relative to the warp direction (see section 5.4).

5.2 Force-to-Stress Conversion

Equation 1 was used to relate the applied force to the stress within the fabric ply. If the applied force were not distributed uniformly across the 50.8-mm width, then the 68 yarns would not have been equally loaded. In this case, equation 1 would yield an average stress across the specimen width and not the actual stress in each yarn. Similarly, in a given yarn all 400 filaments might not have been equally loaded.

Equation 1 makes use of an effective ply thickness, d_o . In evaluating d_o in section 3.2, the cross-sectional area of each filament had to be estimated based on a nominal filament diameter of 12 μm and the assumption of a perfectly circular filament cross section.

5.3 Fabric Strength

For a single ply of Kevlar KM2 style 706, Tables 3 and 4 and Figure 12 show that σ_{fail} varied between 2.08 and 2.34 GPa with a mean of 2.23 GPa in the six warp-direction tests and between 2.62 and 2.78 GPa with a mean of 2.67 GPa in the six fill-direction tests. These results can be compared with values in the literature.

Johnson et al. (1999) reported a strength of 3.34 GPa for a single ply of plain-woven 850-denier KM2 (style 705). They do not specify whether their specimen was loaded in the warp or fill direction, nor do they specify any details of the experimental procedure. (The focus of their paper is on the development of a fabric constitutive model and not on the experimentally obtained input to the model.) This value of 3.34 GPa is substantially larger than both the warp

and fill values in Tables 3 and 4, respectively, for a ply of plain-woven 600-denier KM2 (style 706). Whether this discrepancy originates in real differences between the two batches of specimens or in experimental error cannot be determined. Note that 850- and 600-denier KM2 differ only in the number of filaments per yarn. Since the number of filaments per yarn was taken into account in the normalization procedure of obtaining stress from force, the distinction between 850 and 600 denier cannot account for the discrepancy.

The authors know of no other stiffness value reported in the literature for woven KM2 fabric. However, Yang (2000) reports a yarn strength of 3.3 GPa for KM2. This exceeds the 2.23-GPa mean warp-direction value (Table 3) by 34% and the 2.67-GPa mean fill-direction value (Table 4) by 19%. Substantial degradation in yarn strength is known to occur in the weaving and fixing processes (Scott 2001), so that these substantial differences between fabric strength and prewoven yarn strength are plausible. Another consideration is that the single-yarn specimen studied in Yang (2000) may have been helically twisted prior to testing, whereas yarns in woven fabric are generally untwisted.

5.4 Failure Conditions for Warp vs. Fill Directions

Tables 3 and 4 and Figures 12–14 show smaller fabric strength, σ_{fail} , greater displacement at failure, Δx_{fail} , and smaller work at failure (toughness), W_{fail} , in the warp-direction tests relative to the fill-direction tests. Since, in the weaving process, adjacent warp yarns are respectively raised and lowered to accommodate a fill yarn, warp yarns initially have more slack, or crimp, than fill yarns. Hence, one would expect a greater Δx_{fail} under tensile loading in the warp direction than in the fill direction because more Δx goes into uncrimping yarns in the former case. The observation that σ_{fail} and W_{fail} were smaller in the warp direction than in the fill direction can most likely be attributed to a greater mechanical degradation incurred by the warp yarns during the weaving and/or finishing processes.

5.5 Bilinear vs. Exponential vs. Quartic Fits to Stress-Displacement Curves

Figure 36 collects ε results from bilinear, exponential, and quartic fits to warp data, and the values are listed in Tables 5, 7, and 9. Figure 37 does the same for fits to fill data and the values are listed in Tables 6, 8, and 10.

The exponential form, with only two parameters, is generally a better fit to warp data than is the three-parameter bilinear form (although there is some overlap). On the other hand, the bilinear form generally provides a better fit to fill data than the exponential form. In the case of stress-strain curves for woven cotton fabrics, Jinlian and Newton (1993) found the exponential fit superior to the bilinear fit in both the warp and the fill directions.

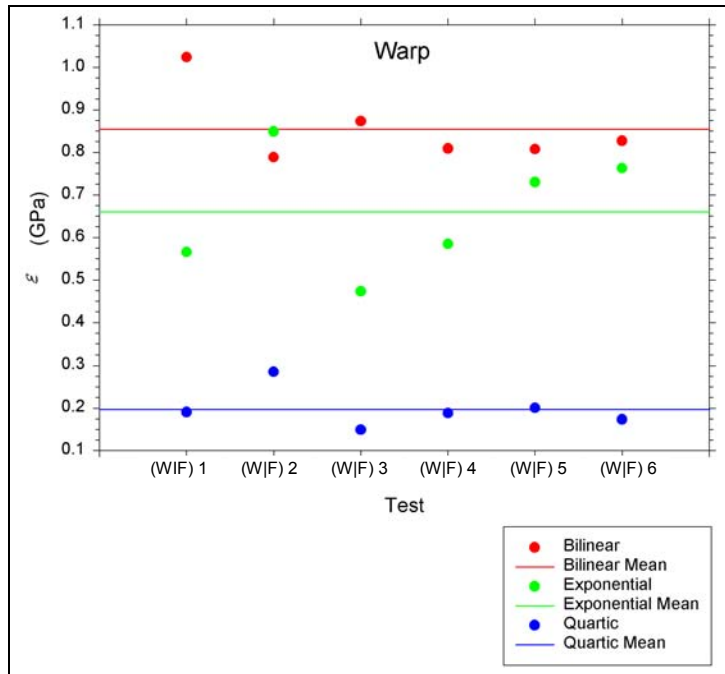


Figure 36. Least-squares errors for the bilinear, exponential, and quartic fits to the warp-direction fabric stress-crosshead displacement curves.

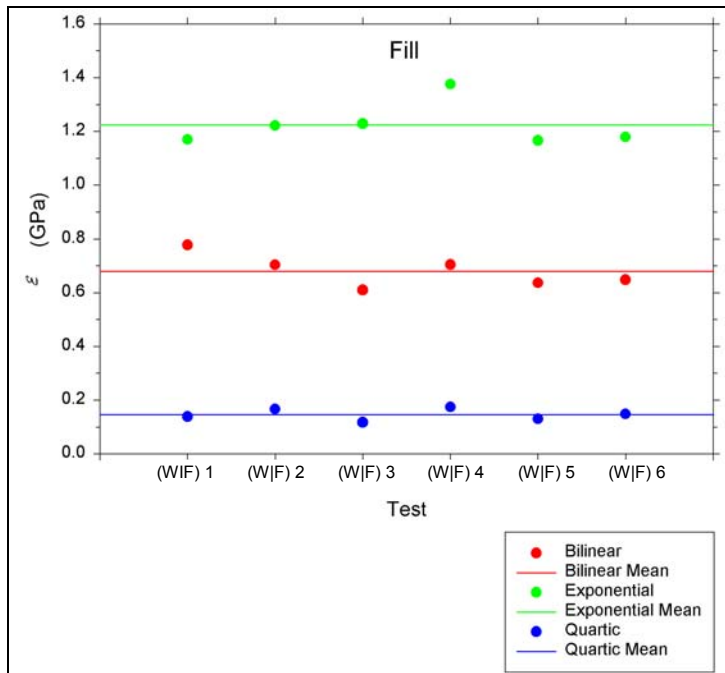


Figure 37. Least-squares errors for the bilinear, exponential, and quartic fits to the fill-direction fabric stress-crosshead displacement curves.

Visual comparison of the four-parameter quartic fits in Figures 34 and 35 with the bilinear fits in Figures 22 and 23 and the exponential fits in Figures 27 and 28 reveals the quartic fit to be the closest, at least for tests W1 and F1. The observation that the quartic fit is the closest for the other tests as well is borne out by Figures 36 and 37. Here, all quartic values for ϵ are smaller than any bilinear or exponential value. The quartic fit has apparently not been proposed previously in the fabric literature.

This observation of a close fit obtainable with a quartic can most likely be transferred from fabric stress-crosshead displacement curves to fabric stress-fabric strain curves. However, this transferability might not be the case if the effective gauge length varies during the course of a test since this would alter the shape of the stress-strain curve relative to the stress-displacement curve.

Computationally, the quartic fit should not be substantially more expensive to evaluate than the exponential fit. These should both be less expensive than the bilinear fit, which requires a check on the current strain level relative to Δx_{lock} .

6. Concluding Remarks

6.1 Summary of Results

Quasi-static, uniaxial tension tests were conducted on 50.8-mm-wide single-ply specimens of plain-woven Kevlar KM2 fabric (style 706.) Six specimens were pulled along the warp direction, and six were pulled along the fill direction. Fabric stress-crosshead displacement results were presented from each test (Figures 6 and 7). The strength (maximum stress achieved) was found to range from 2.07 to 2.33 GPa with a mean of 2.23 GPa in the warp direction and from 2.47 to 2.77 GPa with a mean of 2.67 GPa in the fill direction (Tables 3 and 4 and Figure 12).

Three least-square-error fits were obtained to the fabric stress-crosshead displacement curve from each test: (1) bilinear, (2) exponential, and (3) quartic. For both warp and fill data, the quartic fits were generally the closest.

6.2 Recommendations for Future Work

In the present study, it was not possible to determine fabric strain from crosshead displacement because the effective gauge length was undetermined. The experiments should be repeated using an electromechanical extensometer or an optical technique to measure local fabric deformation over a known initial gauge length. A challenge with the former approach is the need to grip the fabric specimen without inflicting damage.

The tests were performed at a single small crosshead displacement rate, producing quasi-static results. In ballistic impact much larger loading rates are achieved. An Instron or MTS Systems Corp. machine would allow for examination of strain rate dependence over a modest range. A Kolsky bar approach (Shim et al. 2001) would allow still larger strain rates to be achieved.

7. References

- American Society for Testing and Materials (ASTM). "Standard Test Method for Breaking Force and Elongation of Textile Fabrics (Strip Method)." ASTM D5035-95, West Conshohocken, PA, July 1995.
- Alsawaf, F. B. Ph.D. Thesis. University of Manchester, Manchester, UK, 1985.
- E. I. du Pont de Nemours and Company. "Kevlar KM2, Preliminary Information Bulletin." Wilmington, DE, undated.
- Grosberg, P. "The Tensile Properties of Woven Fabrics." *Structural Mechanics of Fibers, Yarns, and Fabrics*. Volume 1, edited by J. W. S. Hearle, P. Grosberg, and S. Backer, New York: Wiley-Interscience, pp. 339–354, 1969.
- Instron Corporation. "The Series 4500 Floor Model Load Frames." Manual no. M10-4500-51, issue B, Canton, MA, June 1988.
- Jinlian, H., and A. Newton. "Modeling of Textile Stress-Strain Curve of Woven Fabrics." *Journal of China Textile University (English Edition)*, vol. 10, no. 4, 1993.
- Johnson, G. R., S. R. Beissel, and P. M. Cunniff. "A Computational Model for Fabrics Subjected to Ballistic Impact." *18th International Symposium on Ballistics*, vol. 2, edited by W. G. Reinecke, Lancaster, PA: Technomic Publishing, pp. 962–969, 1999.
- Malvern, L. E. *Introduction to the Mechanics of a Continuous Medium*. Englewood Cliffs, NJ: Prentice-Hall, 1969.
- National Institute of Justice. *Ballistic Resistance of Police Body Armor*. NIJ Standard 0101.03, U.S. Department of Justice, Washington, DC, April 1987.
- Scott, B. R. Personal communication with M. Raftenberg. E. I. du Pont de Nemours and Company, Wilmington, DE, 2001.
- Shim, V. P. W., C. T. Lim, and K. J. Foo. "Dynamic Mechanical Properties of Fabric Armour." *International Journal of Impact Engineering*, vol. 25, pp. 1–15, 2001.
- Warner, S. B. *Fiber Science*. Englewood Cliffs, NJ: Prentice-Hall, 1995.
- Yang, H. H. *Kevlar Aramid Fiber*. Chichester, UK: John Wiley, 1993.

Yang, H. H. "Aramid Fibers." *Comprehensive Composite Materials, Volume 1, Fiber Reinforcements and General Theory of Composites*, Oxford, UK: Elsevier Science, pp. 199–229, 2000.

List of Symbols

E_y	single-yarn stiffness
F	force exerted on the specimen
N	the value of i corresponding to σ_{fail}
W	work per unit undeformed cross-sectional area
W_{fail}	work at failure per unit cross-sectional area
d_o	initial effective thickness of the fabric specimen
$e_{y,fail}$	engineering strain at failure in a single-yarn specimen
t	time
i	index identifying a particular data point ($\Delta x_i, \sigma_i$)
w_o	initial width of the fabric specimen
x	distance between the loading frame's moving and stationary crossheads
ΔL	elongation of the fabric specimen from its initial length
Δx	displacement of loading-frame crosshead
Δx_N	N^{th} measured crosshead displacement
Δx_{fail}	displacement of loading-frame crosshead at fabric failure
Δx_i	the i^{th} measured crosshead displacement
Δx_{lock}	locking displacement for the bilinear fit to a stress-displacement curve
α	linear-term coefficient in the quartic fit to a stress-displacement curve
β	quadratic-term coefficient in the quartic fit to a stress-displacement curve
β_1	small-displacement slope for the bilinear fit to a stress-displacement curve
β_2	large-displacement slope for the bilinear fit to a stress-displacement curve

γ	cubic-term coefficient in the quartic fit to a stress-displacement curve
δ	quartic-term coefficient in the quartic fit to a stress-displacement curve
ϵ	least-squares error associated with a fit to a stress-displacement curve
ξ, η	exponential-fit parameters
σ	First Piola-Kirchhoff axial stress (engineering stress)
σ_{fail}	strength of a fabric specimen
σ_i	stress corresponding to displacement Δx_i

REPORT DOCUMENTATION PAGE			Form Approved OMB No. 0704-0188
Public reporting burden for this collection of information is estimated to average 1 hour per response, including the time for reviewing instructions, searching existing data sources, gathering and maintaining the data needed, and completing and reviewing the collection of information. Send comments regarding this burden estimate or any other aspect of this collection of information, including suggestions for reducing this burden, to Washington Headquarters Services, Directorate for Information Operations and Reports, 1215 Jefferson Davis Highway, Suite 1204, Arlington, VA 22202-4302, and to the Office of Management and Budget, Paperwork Reduction Project(0704-0188), Washington, DC 20503.			
1. AGENCY USE ONLY (Leave blank)	2. REPORT DATE December 2002	3. REPORT TYPE AND DATES COVERED Final, June 2001-July 2002	
4. TITLE AND SUBTITLE Quasi-Static Uniaxial Tension Characteristics of Plain-Woven Kevlar KM2 Fabric		5. FUNDING NUMBERS 1L162618AH80	
6. AUTHOR(S) Martin N. Raftenberg and Thomas J. Mulkern			
7. PERFORMING ORGANIZATION NAME(S) AND ADDRESS(ES) U.S. Army Research Laboratory ATTN: AMSRL-WM-TD Aberdeen Proving Ground, MD 21005-5066		8. PERFORMING ORGANIZATION REPORT NUMBER ARL-TR-2891	
9. SPONSORING/MONITORING AGENCY NAME(S) AND ADDRESS(ES)		10. SPONSORING/MONITORING AGENCY REPORT NUMBER	
11. SUPPLEMENTARY NOTES			
12a. DISTRIBUTION/AVAILABILITY STATEMENT Approved for public release; distribution is unlimited.		12b. DISTRIBUTION CODE	
13. ABSTRACT (Maximum 200 words) Quasi-static uniaxial tension tests were conducted on 50.8-mm-wide single-ply specimens of plain-woven DuPont Kevlar KM2 aramid fabric (style 706). Six specimens were pulled along the warp direction, and six were pulled along the fill direction. The strength was found to range from 2.07 to 2.33 GPa, with a mean of 2.23 GPa in the warp direction and from 2.47 to 2.77 GPa, with a mean of 2.67 GPa in the fill direction. A bilinear, an exponential, and a quartic fit were obtained to the fabric stress-crosshead displacement curve from each test, with the quartic fit generally found to be the closest.			
14. SUBJECT TERMS Kevlar, KM2, personnel protection, body armor, mechanical properties, constitutive properties, fabric		15. NUMBER OF PAGES 40	
		16. PRICE CODE	
17. SECURITY CLASSIFICATION OF REPORT UNCLASSIFIED	18. SECURITY CLASSIFICATION OF THIS PAGE UNCLASSIFIED	19. SECURITY CLASSIFICATION OF ABSTRACT UNCLASSIFIED	20. LIMITATION OF ABSTRACT UL

NSN 7540-01-280-5500

35

Standard Form 298 (Rev. 2-89)
Prescribed by ANSI Std. Z39-18 298-102

<u>NO. OF COPIES</u>	<u>ORGANIZATION</u>
2	DEFENSE TECHNICAL INFORMATION CENTER DTIC OCA 8725 JOHN J KINGMAN RD STE 0944 FT BELVOIR VA 22060-6218
1	COMMANDING GENERAL US ARMY MATERIEL CMD AMCRDA TF 5001 EISENHOWER AVE ALEXANDRIA VA 22333-0001
1	INST FOR ADVNCD TCHNLGY THE UNIV OF TEXAS AT AUSTIN 3925 W BRAKER LN STE 400 AUSTIN TX 78759-5316
1	US MILITARY ACADEMY MATH SCI CTR EXCELLENCE MADN MATH THAYER HALL WEST POINT NY 10996-1786
1	DIRECTOR US ARMY RESEARCH LAB AMSRL D DR D SMITH 2800 POWDER MILL RD ADELPHI MD 20783-1197
1	DIRECTOR US ARMY RESEARCH LAB AMSRL CS IS R 2800 POWDER MILL RD ADELPHI MD 20783-1197
3	DIRECTOR US ARMY RESEARCH LAB AMSRL CI OK TL 2800 POWDER MILL RD ADELPHI MD 20783-1197
3	DIRECTOR US ARMY RESEARCH LAB AMSRL CS IS T 2800 POWDER MILL RD ADELPHI MD 20783-1197

<u>NO. OF COPIES</u>	<u>ORGANIZATION</u>
	<u>ABERDEEN PROVING GROUND</u>
2	DIR USARL AMSRL CI LP (BLDG 305)

<u>NO. OF COPIES</u>	<u>ORGANIZATION</u>	<u>NO. OF COPIES</u>	<u>ORGANIZATION</u>
6	US ARMY NATICK SOLDIER CTR P CUNNIFF R KINNEY M LARRIVÉE J F MACKIEWICZ S WACLAWIK J WARD 15 KANSAS ST NATICK MA 01760	2	NORTHWESTERN UNIVERSITY MECHANICAL ENGINEERING H D ESPINOSA W K LIU EVANSTON IL 60208
2	PM SOLDIER SYS W BROWER S PINTER 10125 KINGMAN RD FT BELVOIR VA 22060-5820	1	UNIV OF MISSOURI ROLLA CIVIL ENGINEERING DEPT W SCHONBERG ROLLA MO 65409-0030
1	NATIONAL INST OF JUSTICE S NEWETT 810 SEVENTH ST NW WASHINGTON DC 20531	1	JHU MECH ENG K T RAMESH LATROBE HALL 3400 N CHARLES ST BALTIMORE MD 21218
3	ARMY HPC CENTER S BEISSEL T J HOLMQUIST G R JOHNSON 1200 WASHINGTON AVE SOUTH MINNEAPOLIS MN 55415	1	MIT MATERIALS SCI AND ENG DEPT D ROYLANCE CAMBRIDGE MA 02139
1	NATIONAL INST OF JUSTICE OFFICE OF LAW ENFORCEMENT K HIGGINS BLDG 225 RM A323 GAITHERSBURG MD 20899	1	BROWN UNIVERSITY ENGINEERING R J CLIFTON PROVIDENCE RI 02912
1	UNIV OF MASSACHUSETTS TEXTILE SCIENCES S B WARNER NORTH DARTMOUTH MA 02747	1	SRI INTERNATIONAL D SHOCKEY 333 RAVENSWOOD AVE MENLO PARK CA 94025-3493
1	VIRGINIA POLYTECHNIC INST IMPACT BIOMECHANICS LAB MECHANICAL ENGINEERING S M DUMA BLACKSBURG VA 24061	2	UC SAN DIEGO MECH AEROSPACE ENGRNG M A MEYERS S NEMAT NASSER 9500 GILMAN DR LA JOLLA CA 92093
1	UNIVERSITY OF ALABAMA ENGINEERING MECHANICS S E JONES PO BOX 870278 TUSCALOOSA AL 34587-0278	1	NORTH CAROLINA STATE UNIV DEPT MECH AND AEROSPACE ENGINEERING M ZIKRY BOX 7910 RALEIGH NC 27695-7910
		1	UNIVERSITY OF CINCINNATI COLLEGE OF ENGINEERING A TABIEI 787 RHODES HALL PO BOX 210070 CINCINNATI OH 45221-0070

<u>NO. OF COPIES</u>	<u>ORGANIZATION</u>
2	CALIFORNIA INST OF TECH AERONAUTICS AND APPLIED MECHANICS M ORTIZ G RAVICHANDRAN PASADENA CA 91125
1	UNIVERSITY OF ROCHESTER MECHANICAL ENGR DEPT D J QUESNEL ROCHESTER NY 14627-0132
1	DYNA EAST CORP W FLIS 3620 HORIZON DRIVE KING OF PRUSSIA PA 19406-2647
1	SOUTHWEST RSRCH INSTITUTE ENGR AND MAT SCI DIV C E ANDERSON 6220 CULEBRA ROAD PO DRAWER 28510 SAN ANTONIO TX 78228-0510
1	UNIV OF TEXAS AT AUSTIN INSTITUTE FOR ADV TECH S BLESS 4030 2 W BRAKER LANE AUSTIN TX 78759
1	MISSION RESEARCH CORP R EISLER 735 STATE ST SANTA BARBARA CA 93102
1	DUPONT ENG B SCOTT 101 BEECH ST PO BOX 80840 WILMINGTON DE 19880-0840
1	APPLIED RESEARCH ASSOCIATES D E GRADY SUITE A 220 4300 SAN MATEO BLVD NE ALBUQUERQUE NM 87110
2	DIR LLNL D LASSILLA TECH LIB PO BOX 808 LIVERMORE CA 94550

<u>NO. OF COPIES</u>	<u>ORGANIZATION</u>
5	DIRECTOR SANDIA NATIONAL LABS R BRANNON L CHHABILDAS E HERTEL M KIPP TECH LIB PO BOX 5800 ALBUQUERQUE NM 87185-5800
3	DIR LANL G T GRAY TECH LIB PO BOX 166 LOS ALAMOS NM 87454
1	US ARMY NGIC T SHAVER 2055 BOULDERS RD CHARLOTTESVILLE VA 22911-8318
<u>ABERDEEN PROVING GROUND</u>	
1	COMMANDER US ARMY ATC CSTE DTC AT SL V T E SANDERSON 400 COLLERAN ROAD APG MD 21005-5059
48	DIR USARL AMRSL SL BE E DAVIS D NEADES AMSRL WM J SMITH AMSRL WM M L GHIORSE S GHIORSE E RIGAS G HAGNAUER P MOY D VIECHNICKI AMSRL WM MA S MCKNIGHT AMSRL WM MB T BOGETTI B CHEESEMAN R DOOLEY B FINK G GAZONAS

NO. OF
COPIES ORGANIZATION
ABERDEEN PROVING GROUND (CONT)

D HOPKINS
C HOPPEL
R LIEB
AMSRL WM MC
J LASALVIA
M STAKER
AMSRL WM T
T HAVEL
AMSRL WM TA
W BRUCHEY
M BURKINS
K FRANK
W GILLICH
W GOOCH
T HADUCH
T MOYNIHAN
M NORMANDIA
AMSRL WM TB
N GNIAZDOWSKI
F GREGORY
AMSRL WM TC
K KIMSEY
L MAGNESS
W WALTERS
AMSRL WM TD
T BJERKE
M N RAFTENBERG (6 CPS)
S SCHOENFELD
E RAPACKI
T WEERISOORIYA
M SCHEIDLER
S BILYK
H MEYER
Y HUANG

<u>NO. OF COPIES</u>	<u>ORGANIZATION</u>
1	RAFAEL BALLISTICS CTR M MAYSELESS PO BOX 2250 HAIFA ISRAEL
2	DSTL BIOMEDICAL SCIENCES G COOPER W TAM PORTON DOWN SALISBURY WILTSHIRE SP4 0JQ UNITED KINGDOM
1	DSTO AERONAUTICAL AND MARITIME RESEARCH LABORATORY J J WANG PO BOX 1500 SALISBURY SA 5108 AUSTRALIA
1	DLO R&P P GOTTS SKIMMINGDISH LANE CAVERSFIELD BICESTER OXON OX27 ATS UNITED KINGDOM
1	ARL ERO S SAMPATH AERO MECH ENG 223 MARYLEBONE RD LONDON NW1 5TH UNITED KINGDOM
6	AMC SCI & TECH CTR EUROPE T J MULKERN POSTFACH 81 55247 MAINZ KASTEL GERMANY